Supporting Information for

Two-Dimensional Zr/Hf-Hydroxamate Metal-Organic Frameworks

Qiuxue Lai[1], Zhao-Qin Chu[2], Xinyi Xiao[1], Dejun Dai[3], Ting Song[1], Tian-Yi Luo[4], Wenlei Tang[1], Xuan Feng[1], Zhiyuan Zhang[1], Tao Li[3], Hai Xiao[5], Jing Su[2]* and Chong Liu[1]*

1. School of Chemical Engineering, Sichuan University, Chengdu, 610065, China
2. College of Chemistry, Sichuan University, Chengdu, 610064, China
3. School of Physical Science and Technology, ShanghaiTech University, Shanghai, 201210, China
4. Institute for NanoBioTechnology, Johns Hopkins University, Baltimore, MD 21218, USA
5. Department of Chemistry, Tsinghua University, Beijing, 100084, China

Contents:

1. General procedures

All purchased chemicals were used without further purification except where otherwise noted. All *N*,*N*-dimethylformamide (DMF) used for washing crystals was pre-dried over 4Å molecular sieves.

Powder X-ray diffraction (PXRD) patterns were collected on a Rigaku MiniFlex600 at 40 kV, 40 mA for Cu Kα, (λ = 1.54178 Å) with a scan speed of 10 º/min from 3 º to 30 º at a step size of 0.01 º. The simulated powder patterns were calculated using Materials Studio based on crystal structures of corresponding MOFs.

Single-crystal X-ray diffraction (SC-XRD) data for SUM-1(Zr) and SUM-1(Hf) were collected on a Bruker D8 Venture single-crystal X-ray diffractometer (Mo Kα radiation, λ = 0.71073 Å) at 120 K and 150 K, respectively. The crystal structures were solved with direct method using SHELXT[1] and refined by full-matrix least-squares on F^2 using SHELXL[2] in Olex2[3]. Refinement details are provided in Tables S1 and S2.

^{1}H NMR spectra were obtained using a JNM-ECZ400S/L1(JEOL Ltd., Japan) 400 MHz spectrometer. Chemical shifts are in parts per million using the residual solvent peak (DMSO-d_6) as the reference.

N_2 adsorption-desorption experiments were performed on a BELSORP MAX instrument at 77 K. Activation procedure is described in Section 6.4.

Optical microscopic images were obtained using a Ruihong BM-500T microscope.

Thermogravimetric analysis (TGA) was carried out on a TA Discovery SDT 650 simultaneous thermal analyzer from room temperature to 600 ºC at a heating rate of 10 ºC/min in a N_2 flow of 100 mL/min.

Scanning electron microscopy (SEM) images were obtained using a JEOL JSM-7610 SEM (Toyoko, Japan) with accelerating voltages of 5.0 kV.

Fourier transform infrared (FTIR) spectra were collected in the range of 400-4000 cm^{-1} on a Spectrum Two Li10014 infrared spectrometer using compressed KBr pellets.

Batch synthesis of MOFs and optimization of synthetic conditions were performed on a custom-made automatic array reactor (Model MOF-64) by Huzhou Lexun Technology Co., Ltd. The reactor provides 8×8 reaction positions (for glass vials) and an automatic

distribution mechanism of liquid reagents/samples that is controlled by software interface.

2. Syntheses of H_2-BDHA, SUM-1(Zr) and SUM-1(Hf)

2.1 Synthesis of benzene-1,4-dihydroxamic acid (H_2-BDHA)

H_2-BDHA was synthesized according to the procedure reported by Griffith et al[4] with minor modification: hydroxylamine hydrochloride (12.6 g, 180 mmol) was mixed with sodium hydroxide (14.4 g, 360 mmol) in deionized water (90 mL). The aqueous solution was then added to a suspension of dimethyl terephthalate (11.6 g, 60 mmol) in methanol (100 mL). The resulting mixture was stirred for 72 hours at 40 ºC before cooling down to room temperature and subsequently acidified to pH 5.5 with a solution of 5% HCl/H_2O (ca. 90 mL). The white solids were collected by filtration and washed successively with deionized H_2O (60 mL), saturated $NaHCO_3$/H_2O (3 × 30 mL) and deionized H_2O (2 × 30 mL). The final product H_2-BDHA was dried in air overnight as white solids (6.4 g, yield: 55%). ^{1}H NMR (400 MHz, DMSO-d_6): 11.31 (brs, 2H), 9.20 (brs, 2H), 7.80(s, 4H), shown in Fig. S1.

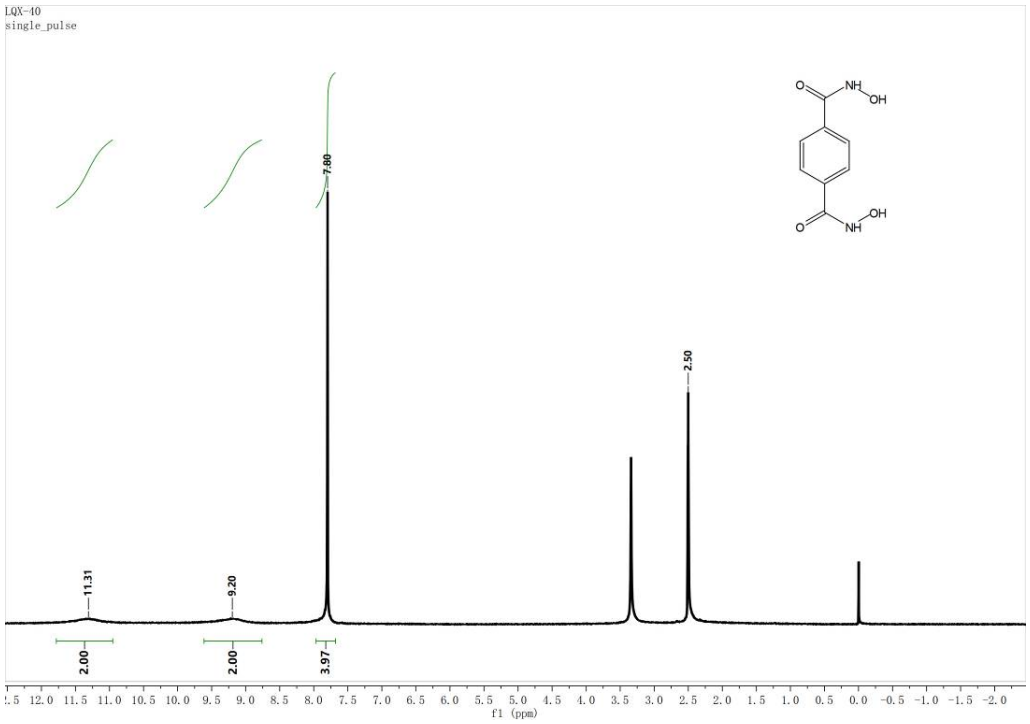

Fig. S1 ^{1}H NMR spectrum of H_2-BDHA in DMSO-d_6.

2.2 Synthesis of SUM-1(Zr)

$ZrCl_4$ was dissolved in DMF (0.03 M, 1 mL) with the aid of ultrasonication. A suspension of H_2-BDHA (0.10 M, 1 mL) was prepared by mixing the ligand with DMF and sonicating for 20 min. In a 4-mL glass vial, the two were mixed and briefly sonicated. The vial was tightly capped and heated in a 120 ºC isothermal oven for 10-40 min. After cooling to room temperature, the crystals were collected and washed with dry DMF.

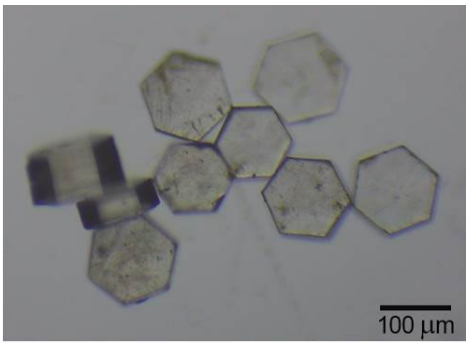

Fig. S2 Optical image of SUM-1(Zr)

2.3 Synthesis of SUM-1(Hf)

$HfCl_4$ was mixed with DMF (0.03 M, 1 mL) and sonicated. A suspension of H_2-BDHA (0.09 M, 1 mL) was prepared by mixing the ligand with DMF and sonicating for 20 min. In a 4-mL glass vial, the two were mixed and briefly sonicated. The vial was tightly capped and heated in a 120 ºC isothermal oven for 40 min. After cooling to room temperature, the crystals were collected and washed with dry DMF.

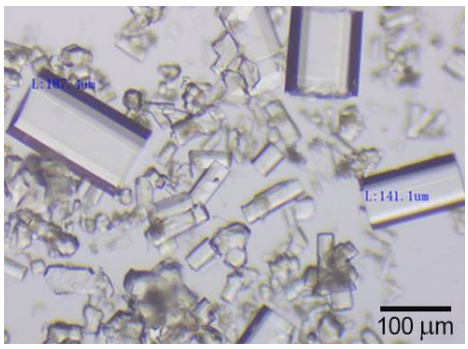

Fig. S3 Optical image of SUM-1(Hf)

3. Crystal structures of SUM-1(Zr) and SUM-1(Hf)

3.1 Crystal structure of SUM-1(Zr)

Table S1 Crystal structure refinement table for SUM-1(Zr)

Identification code	SUM-1Zr	
CCDC deposition number	2121493	
Empirical formula	C16H12N4O8Zr	
Formula weight	479..52	
Temperature	120.0 K	
Crystal system	hexagonal	
Space group	*P6/mmm*	
Unit cell dimensions	*a* = 23.168(2) Å	*α* = 90°
	b = 23.168(2) Å	*β* = 90°
	c = 8.0801(11) Å	*γ* = 120°
Volume	3756.1(9) $Å^3$	
Z	3	
F(000)	720.0	
Crystal size	0.11 × 0.09 × 0.09 mm^3	
Theta range for data collection	4.06 to 54.992	
Index ranges	-27<=h<=30, -30<=k<=29, -9<=l<=10	
Reflections collected	36009	
Independent reflections	1724 [Rint = 0.1500, Rsigma = 0.0507]	
Data / restraints / parameters	1724/0/64	
Goodness-of-fit on F^2	1.080	
Final R indices [I>2sigma(I)]	R1 = 0.0892, wR2 = 0.2487	
R indices (all data)	R1 = 0.1019, wR2 = 0.2633	
Largest diff. peak and hole	1.66 and -1.37e.$Å^{-3}$	

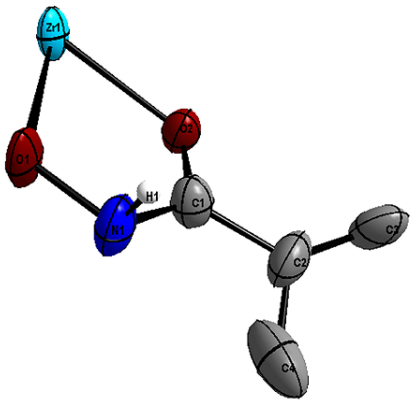

Fig. S4 ORTEP diagram of the asymmetric unit of SUM-1(Zr) (50% probability factor for the thermal ellipsoids), generated in Diamond 3.2k.

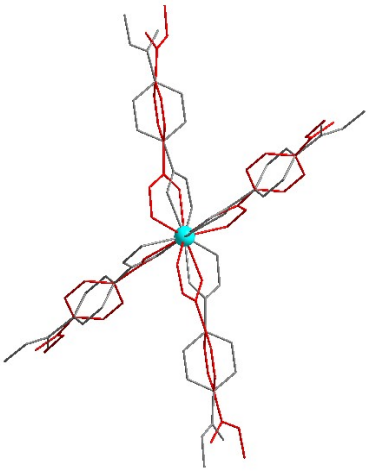

Fig. S5 Model of the codependent disordering in the crystal structure of SUM-1(Zr). The red and gray stick models represent the two conformations of the ligands of equal probability, the blue ball represents the Zr atom.

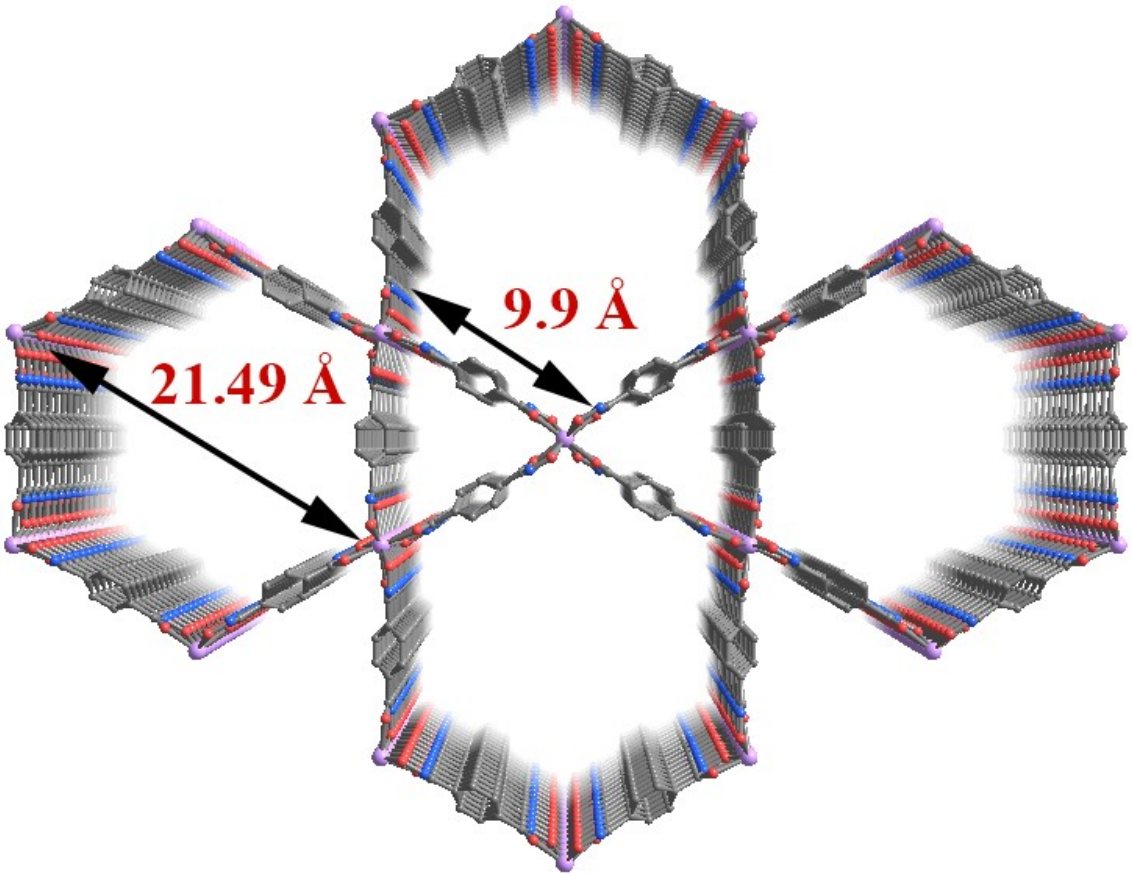

Fig. S6 Crystal structure of SUM-1(Zr) with disorders removed for clarity, in packed mode, viewed along the *c* axis. Zr: purple spheres; C: gray spheres; N: blue spheres; O: red spheres; H: omitted for clarity.

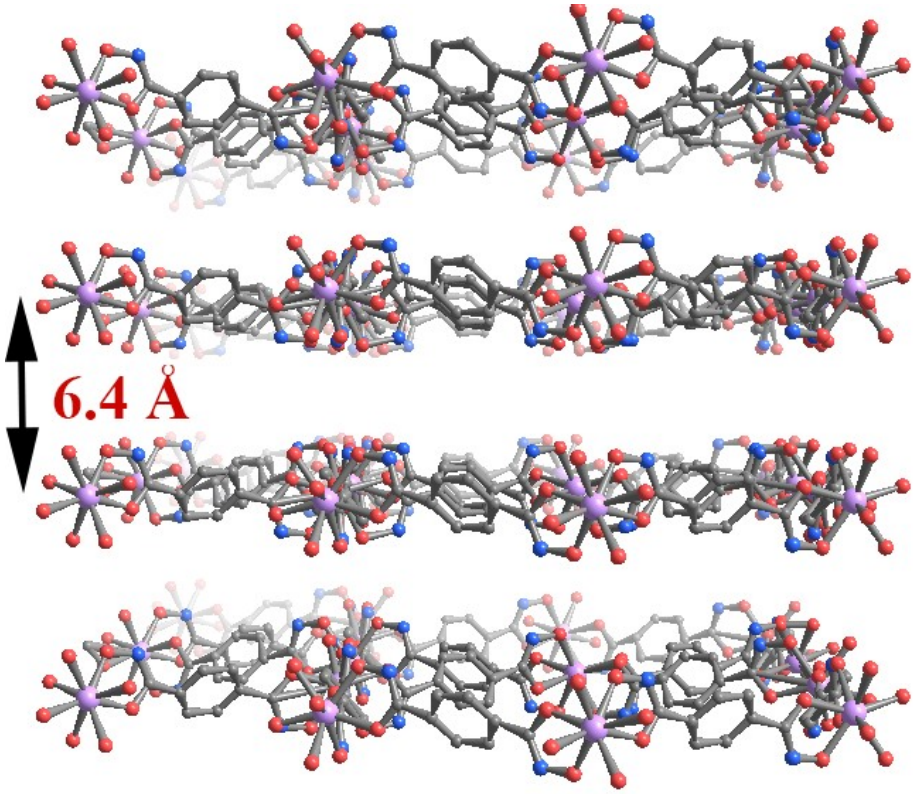

Fig. S7 Crystal structure of SUM-1(Zr) with disorders removed for clarity, in packed mode, viewed along the *a* axis. Zr: purple spheres; C: gray spheres; N: blue spheres; O: red spheres; H: omitted for clarity.

3.2 Crystal structure of SUM-1(Hf)

Table S2 Crystal structure refinement table for **SUM-1(Hf)**

Identification code	SUM-1Hf	
CCDC deposition number	2121494	
Empirical formula	C16H12HfN4O8	
Formula weight	566.79	
Temperature	150.0 K	
Crystal system	hexagonal	
Space group	*P6/mmm*	
Unit cell dimensions	*a* = 23.1152(8) Å	
Unit cell dimensions Volume	*b* = 23.1152(8) Å	*α* = 90°
	c =8.1157(5) Å	*β* = 90°
	3755.4(3) Å^3	*γ* = 120°
Z	3	
F(000)	816.0	
Crystal size	0.08 × 0.02 × 0.02 mm^3	
Theta range for data collection	4.07 to 54.99	
Index ranges	-28<=h<=30, -22<=k<=29, -10<=l<=10	
Reflections collected	33357	
Independent reflections	1723 [Rint = 0.1241, Rsigma = 0.0385]	
Data / restraints / parameters	1723/0/64	
Goodness-of-fit on F^2	1.0580	
Final R indices [I>2sigma(I)]	R1 = 0.0562, wR2 = 0.1386	
R indices (all data)	R1 = 0.0618, wR2 = 0.0.1413	
Largest diff. peak and hole	1.59 and -4.47e.Å^{-3}	

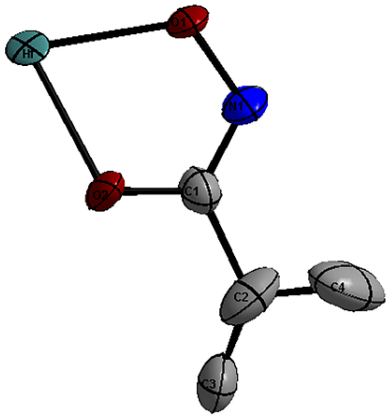

Fig. S8 ORTEP diagram of the asymmetric unit of SUM-1(Hf) (50% probability factor for the thermal ellipsoids), generated in Diamond 3.2k.

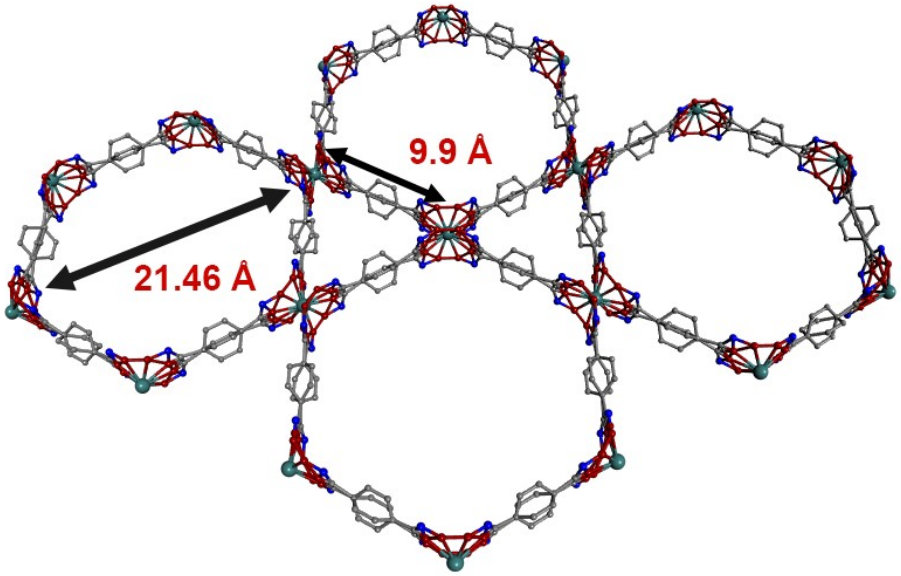

Fig. S9 Crystal structure of SUM-1(Hf) with disorders shown, bird's eye view from the top. Hf: turquoise spheres; C: gray spheres; N: blue spheres; O: red spheres; H: omitted for clarity.

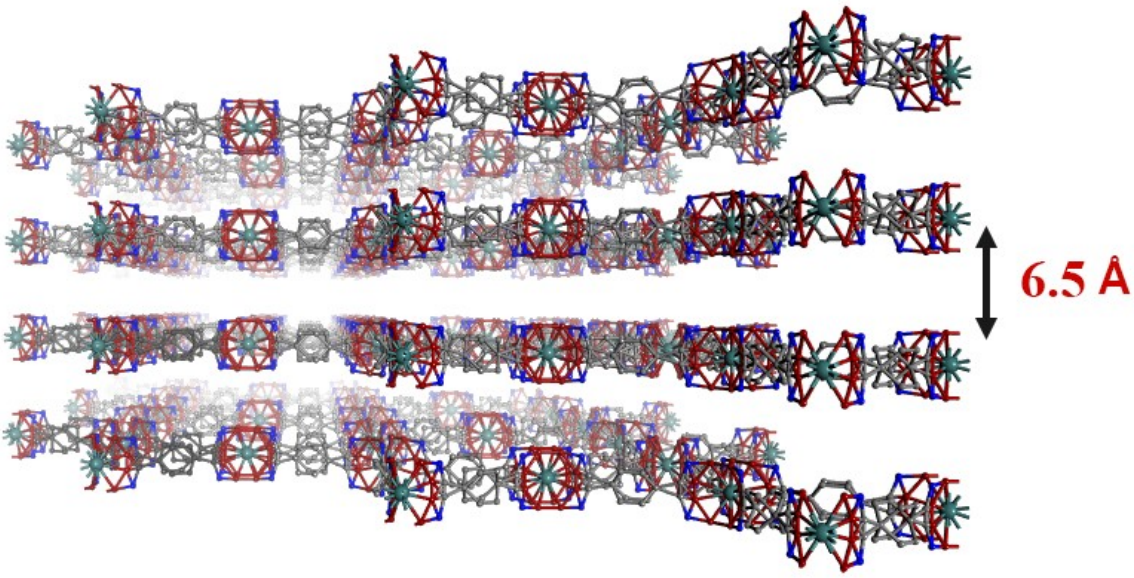

Fig. S10 Crystal structure of SUM-1(Hf) in packed mode with disorders shown, side view. Hf: turquoise spheres; C: gray spheres; N: blue spheres; O: red spheres; H: omitted for clarity.

4. Computational study of Zr-hydroxamate system

Kohn–Sham density functional theory (DFT)[5,6] calculations were performed with the Gaussian 16 program.[7] In this work, the hybrid functional B3LYP[8,9] was used for geometry optimization and harmonic frequency calculations on the mononuclear and dinuclear species of Zr-hydroxamate system in the gas phase. The calculated vibrational frequencies are positive confirming that the fully optimized structures were stationary points on the potential energy surface, and the corresponding thermochemistry corrections to the free energy were obtained. We applied the 6-311G* basis sets[10,11] for C, N, O and H atoms, and Stuttgart energy-consistent relativistic pseudopotential ECP28MWB[12] and the corresponding ECP28MWB-SEG basis for Zr atom.

4.1 Mononuclear species in the Zr-hydroxamate system

In order to understand why the hydroxamate ligand uses two O atoms rather than N and O atoms of the oxime group to coordinate to the Zr atom, as shown in the experimental crystal structure of SUM-1(Zr), we constructed two other possible isomers with N, O coordination and performed geometry optimization and vibrational frequency calculations on these three 8-coordinated mononuclear Zr-hydroxamate complexes i.e., Zr(hydroxamate)$_4$, at DFT/B3LYP level. The optimized geometries of these three isomers are shown in Fig. S11 with the relative energy and average bond lengths compiled in Table S3.

According to Table S3, the isomer M(O_C,O_N) with two O atoms as coordination atoms is much more stable than the cis-/trans-M(N,O_N) complexes using oxime group to coordinate by 37.6 and 51.4 kcal/mol in energy, respectively. This huge energy differences explain why the M(O_C,O_N) complex was readily synthesized without observation of the formation of the other two isomers. Besides, the calculated average Zr-O_C and Zr-O_N bond lengths in M(O_C,O_N) complex are 2.32 and 2.15 Å, respectively, in good agreement with experimental crystal structure data, i.e., 2.21 and 2.16 Å, respectively.

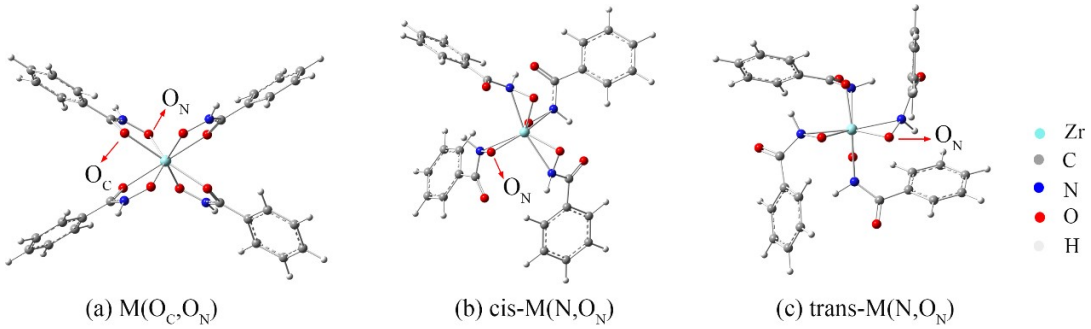

(a) M(O_C,O_N) (b) cis-M(N,O_N) (c) trans-M(N,O_N)

Fig. S11 The DFT/B3LYP optimized geometries of three isomers of 8-coordinated mononuclear Zr-hydroxamate complexes, i.e., Zr(hydroxamate)$_4$: (a) M(O_C, O_N), (b) cis-M(N, O_N), and (c) trans-M(N, O_N).

Table S3 The DFT/B3LYP calculated relative energy (in kcal/mol) and average bond lengths (in Å) of three isomers of 8-coordinated mononuclear Zr-hydroxamate complexes, i.e., Zr(hydroxamate)$_4$.

Isomers	Coordination Atoms	Orientation of O_C and O_N of hydroxamte	Relative Energy	*R*(Zr-O_C)	*R*(Zr-O_N)	*R*(Zr-N)
M(O_C,O_N)	O_C,O_N	cis	0	2.32	2.15	-
cis-M(N,O_N)	N,O_N	cis	37.6	-	2.04	2.48
trans-M(N,O_N)	N,O_N	trans	51.4	-	2.06	2.37

4.2 Dinuclear species in the Zr-hydroxamate system

In order to understand why only the mononuclear complex was formed without observation of any multinuclear ones, we constructed a possible dinuclear Zr-hydroxamate complex with each Zr coordinated by three hydroxamate ligands similar to the mononuclear one and the two Zr atoms connected by another two bridging hydroxamate ligands using two O atoms as the ends of the bridge (Fig. S12). Due to the different orientations of two benzene rings of the two bridging hydroxamate ligands, there are two isomers, i.e., D-is1 and D-is2, with C_2 and C_1 symmetry, respectively, for this dinuclear complex (see Fig. S12 for the DFT/B3LYP optimized structures). In these two isomers, each Zr atom has the same coordination environment and is coordinated by eight O atoms. The calculated relative energy and average bond lengths are summarized in Table S4. These two isomers have very similar average terminal and bridging Zr-$O_{C/N}$ bond lengths with the difference no larger than 0.02 Å. As the D-is1 isomer of C_2 symmetry is 8.5 kcal/mol more stable than that of D-is2 one of C_1 symmetry in energy. Therefore, the C_2-symmetry dinuclear complex is used in the following thermodynamic analysis and discussion. Compared to the mononuclear complex M(O_C,O_N), the dinuclear complex D-is1 has a slightly longer average terminal Zr-O_C bond by ~0.05 Å and a similar average terminal Zr-O_N bond length with the difference of 0.01 Å.

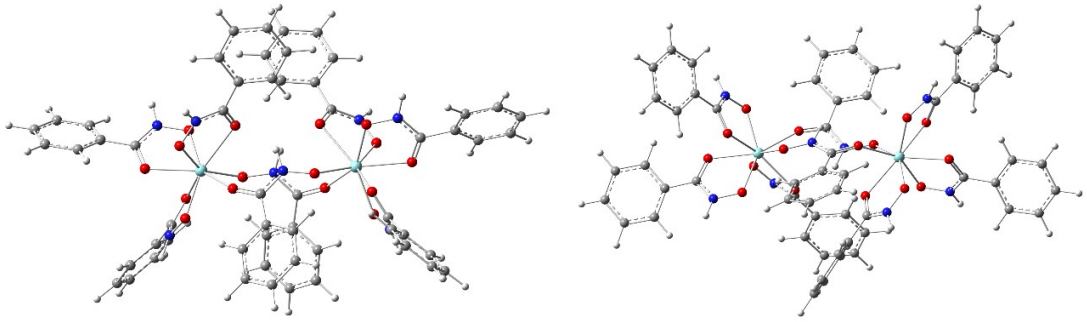

(a) D-is1 (C_2 symmetry) (b) D-is2 (C_1 symmetry)

Fig. S12 The DFT/B3LYP optimized geometries of two isomers of dinonuclear Zr-hydroxamate complexes, i.e., Zr_2(hydroxamate)$_8$: (a) D-is1 (C_2 symmetry) and (b) D-is2 (C_1 symmetry).

Table S4 The DFT/B3LYP calculated relative energy (in kcal/mol) and average bond lengths (in Å) of two isomers of the dinuclear Zr-hydroxamate complexes, i.e., Zr_2(hydroxamate)$_8$.

Isomers	Symmetry	Relative Energy	Terminal *R*(Zr-O_C)	Terminal *R*(Zr-O_N)	Bridging *R*(Zr-O_C)	Bridging *R*(Zr-O_N)
D-is1	C_2	0	2.39	2.14	2.27	2.11
D-is2	C_1	8.5	2.38	2.14	2.29	2.12

4.3 Thermodynamic analysis of formation of the dinuclear complex from two mononuclear complexes in the Zr-hydroxamate system

The Gibbs free energy (*G*) is an important parameter in thermodynamic processes and is often used to predict whether a reaction will occur spontaneously. We calculated the Gibbs free energy change (ΔG) of the formation reaction of dinuclear complex from two mononuclear complexes in the Zr-hydroxamate system, which is defined as:

$$\Delta G = G_{dinu} - 2G_{mononu} \qquad (1)$$

Where G_{dinu} is the *G* of the dinuclear complex D-is1 of C_2 symmetry and G_{mononu} is the *G* of the mononuclear complex, M(O_C,O_N). The ΔG was calculated to be 18.9 kcal/mol. This huge positive ΔG value shows that the formation of dinuclearity is not thermodynamically favored in the Zr-hydroxamate system, consistent with the experimental observation of sole mononuclear Zr-hydroxamate product.

4.4 Comparison between original and model mononuclear/dinuclear complexes by replacing phenyl group of hydroxamate ligand with hydrogen or methyl group

In order to reduce the computational cost of the subsequent kinetic study on the formation of the dinuclear complex from the mononuclear complex, we constructed two model mononuclear/dinuclear complexes by replacing the phenyl group of hydroxamate ligand with hydrogen or methyl group based on the original one. The DFT/B3LYP optimized geometries of these two types of model complexes were shown in Fig. S13 with the average Zr-$O_{C/N}$ bond lengths in Table S5. Compared to the original mononuclear complex, hydrogen and methyl group substitution give slight longer Zr-O_C

bond by 0.03-0.04 Å and shorter Zr-O_N bond by 0.02 Å. Similarly, the model dinuclear complexes also have similar average terminal Zr-$O_{C/N}$ and bridging Zr-O_N bond lengths as the original one while with a slightly longer bridging Zr-O_C bond by ~0.07 Å. Besides, the ΔG values in equation 1 corresponding to the formation of dinuclear complexes are very positive, i.e., 10.1 and 13.1 kcal/mol for the model system with hydrogen and methyl substitution, respectively, consistent with the result for the original system. This demonstrates the reasonability of using model complexes in the subsequent kinetic study. As these two model complexes do not show significant differences in Zr-$O_{C/N}$ bond lengths and ΔG values, we choose the model complex with hydrogen substitution in the kinetic study to further reduce the computational cost.

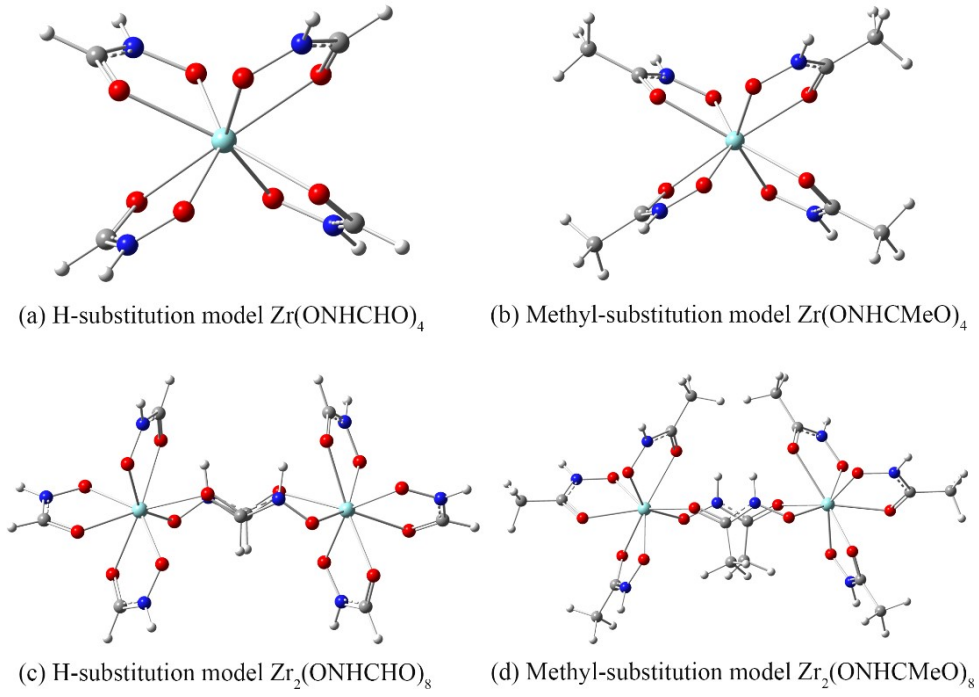

Fig. S13. The DFT/B3LYP optimized model mononuclear/dinuclear complexes by replacing phenyl group of hydroxamate ligand with (a) and (c) hydrogen or (b) and (d) methyl group.

Table S5 The average coordinated bond lengths (in Å) of model mononuclear/dinuclear complexes with hydrogen or methyl substitution of phenyl groups of hydroxamate ligand in the original mononuclear/dinuclear complexes in the Zr-hydroxamate system.

Mononuclear/Dinuclear Complex	Terminal R(Zr-O_C)	Terminal R(Zr-O_N)	Bridging R(Zr-O_C)	Bridging R(Zr-O_N)
Original M(O_C,O_N), $Zr(ONHCPhO)_4$	2.32	2.15	-	-
H-substitution model, $Zr(ONHCHO)_4$	2.36	2.13	-	-
Methyl-substitution model, $Zr(ONHCMeO)_4$	2.35	2.13	-	-
Original D-is1, $Zr(ONHCPhO)_8$	2.39	2.14	2.24	2.11
H-substitution model, $Zr_2(ONHCHO)_8$	2.36	2.14	2.32	2.11
Methyl-substitution model, $Zr_2(ONHCMeO)_8$	2.38	2.14	2.30	2.10

4.5 Kinetic study of the formation of dinuclear complex from two mononuclear complexes based on hydrogen-substitution model system

In order to estimate the reaction barrier of formation of dinuclear complex from two mononuclear complexes in the Zr-hydroxamate system, linear transit (LT) calculations were performed by constrained optimization at each LT coordinate along the $(ONHCHO)_4Zr\cdots Zr(ONHCHO)_4$ dissociation pathway at DFT/B3LYP level. The optimized geometry of the stable dinuclear $Zr_2(ONHCHO)_8$ complex give a distance of 6.716 Å between two Zr atoms. The LT coordinate is defined as the $(ONHCHO)_4Zr\cdots Zr(ONHCHO)_4$ distance $R_n=R_0+1.0n$ (n=0,1,…7), where R_0=6.716 Å corresponding to the stable dinuclear $Zr_2(ONHCHO)_8$ complex. The calculated LT energy curve with the energy of the stable dinuclear $Zr_2(ONHCHO)_8$ complex as reference zero is shown in Fig. S14 together with the geometrical structures at n=0, 2, 7.

The energy curve firstly goes up, and reaches the maximum at n=2, and then goes down, and finally becomes horizontal at n≥6. Obviously, the corresponding structures at n=0, 2, 7 can tell us that the dinuclear complex with each Zr being eight-coordinated gradually dissociates into two seven-coordinated mononuclear complex far apart from each other. According to the calculated energy results, the above dissociation requires an activation energy of 9.9 kcal/mol. Accordingly, the reverse process, i.e., the formation of dinuclear complex from two seven-coordinated mononuclear complexes, need overcome a much larger energy barrier with a value of 21.2 kcal/mol.

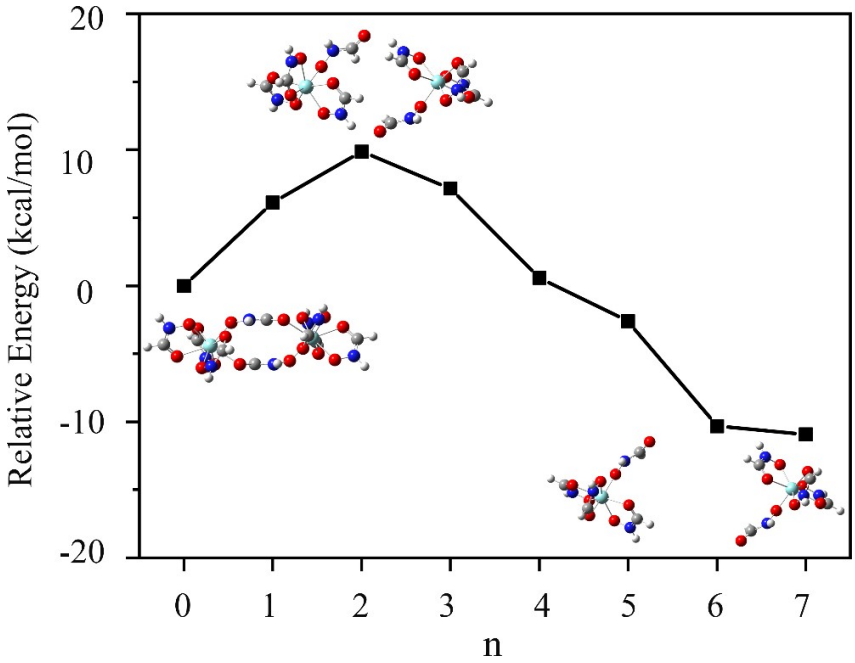

Fig. S14 Linear transit (LT) energy curves illustrating dissociation of $Zr_2(ONHCHO)_8 \rightarrow$ 2 $\{Zr(ONHCHO)_4\}$. Energies are obtained from DFT/B3LYP calculations. The LT coordinate is defined as the $(ONHCHO)_4Zr\cdots Zr(ONHCHO)_4$ distance $R_n=R_0+1.0n$ (n=0,1,…7), where R_0=6.716 Å corresponding to the stable dinuclear $Zr_2(ONHCHO)_8$ complex. The structures at n=0, 2, 7 are given in this figure.

4.6 Kinetic study of transition from eight-coordinated mononuclear complex to seven-coordinated

The LT calculations on the dissociation of dinuclear $Zr_2(ONHCHO)_8$ complex in Fig. S14 give the seven-coordinated mononuclear product but not the most stable eight-coordinated one. Therefore, similar LT calculations were also performed by constrained optimization along the pathway of one coordinated ligand carbonyl oxygen (O_C) departing from Zr metal center, i.e., Zr-O_C distance increasing direction, at DFT/B3LYP to estimate the reaction barrier of the transition from the eight-coordinated mononuclear complex to the seven-coordinated one in the Zr-hydroxamate system. The LT coordinate is defined as the distance between departing Oc and Zr, $d_n=d_0+0.3355n$ (n=0,1,…7), where d_0=2.362 Å. The complexes at the starting and end point, i.e., d(Zr-O_C)=2.362 and 4.711 Å, respectively, correspond to the fully optimized eight-coordinated mononuclear complex and seven-coordinated one as shown in Fig. S15. It is worth mentioning that the initial geometry of seven-coordinated mononuclear complex used for the full optimization calculations is taken out from the dissociation product of the dinuclear species, i.e., the structure at n=7 in Fig. S14.

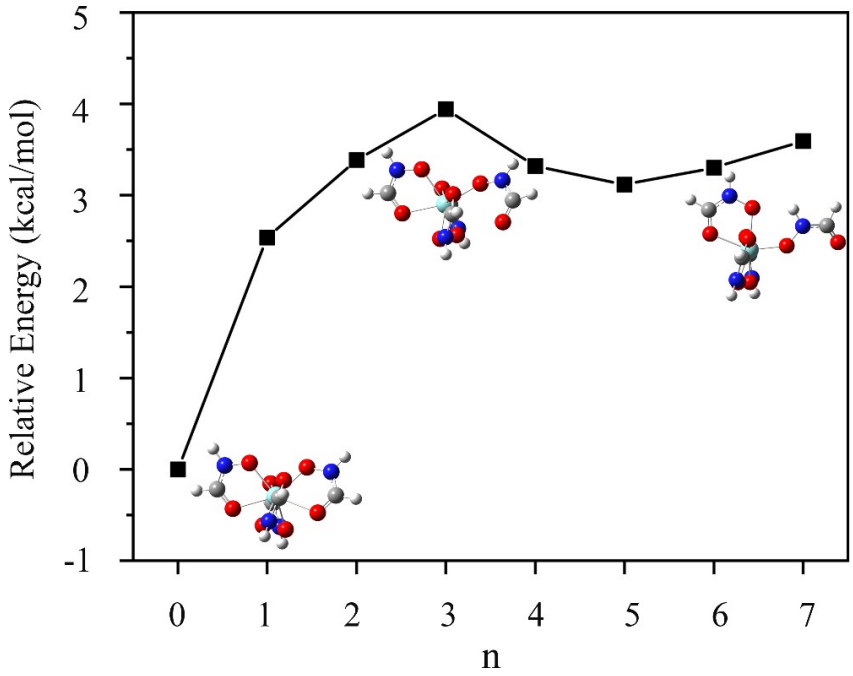

Fig. S15. Linear transit (LT) energy curves illustrating the transition from eight-coordinated mononuclear complex to the seven-coordinated one. Energies are obtained by constrained optimization at each LT coordinate along the pathway of one coordinated ligand carbonyl oxygen (O_C) departing from Zr metal center at DFT/B3LYP level. The LT coordinate is defined as the distance between departing O_C and Zr, $d_n=d_0+0.3355n$ (n=0,1,…7), where d_0=2.362 Å. The complexes at the starting and end point, i.e., d(Zr-O_C)=2.362 and 4.711 Å, respectively, correspond to the fully optimized eight-coordinated mononuclear complex and seven-coordinated one. The structures at n=0, 3, 7 are given in this figure.

The calculated LT energy curve with the energy of the stable eight-coordinated mononuclear model complex $Zr(ONHCHO)_4$ in Table S3 as reference zero is displayed in Fig. S15 together with the geometrical structures at n=0, 3, 7. The energy curve generally goes up till the end point with a maximum at n=3. This clearly shows that seven-coordination is unstable compared to the eight-coordination and the transition from the eight- to seven-coordination by breaking one Zr-O_C bond requires absorbing 3.9 kcal/mol of energy. Combining with the energy curve in Fig. S14, it is estimated that

an overall activation energy of 25.1 kcal/mol is required to form a dinuclear complex from two eight-coordinated mononuclear complexes.

Table S6 Cartesian coordinates (in Å) of DFT/B3LYP optimized geometries of mononuclear and dinuclear species.

M(O_C,O_N), Zr(ONHCPhO)$_4$				**cis-M(N,O_N), cis-Zr(ONHCPhO)$_4$**			
O	-1.86258600	1.22668000	0.63988100	O	-0.04089000	0.57194600	0.64460600
O	1.84950400	-1.25617800	0.67700100	O	-0.03589300	-1.84237500	-2.00872200
O	1.88994300	1.15543600	-0.66362100	O	1.69665600	1.02196700	-2.12953500
O	-1.88175200	-1.22696400	-0.61028500	O	-1.18765600	1.26785300	-2.37770000
O	0.68871100	-1.25141400	-1.60367700	N	-0.10498500	-2.21987600	-0.65695000
N	1.87303200	-1.87780400	-1.44627000	C	-1.30473200	-2.84839900	-0.22776700
H	2.29293500	-2.24555900	-2.28702400	N	0.11208700	1.94366200	0.76855400
C	2.43328200	-1.88705500	-0.24573900	C	1.31655400	2.50220300	1.03152900
O	-0.69452900	1.17003800	-1.63430400	N	-2.21759900	0.56517600	-1.71460200
N	-1.87309800	1.81189900	-1.49414800	C	-3.00530000	1.31655900	-0.80439500
H	-2.16646200	2.36815000	-2.28375500	N	2.39030700	0.18298300	-1.22658100
C	-2.44265600	1.83745000	-0.29760400	Zr	0.09471800	0.07316800	-1.33266800
O	-0.72517700	-1.17593100	1.66893500	O	-2.29829200	-2.85736000	-0.91704100
N	-1.91336600	-1.79784800	1.52763100	O	-2.58012000	2.33768700	-0.30546800
H	-2.21607000	-2.34954300	2.31707400	O	2.36389500	1.84880900	1.08264800
C	-2.47687700	-1.82257400	0.32849400	O	3.30767200	-0.99823900	-2.97087500
O	0.72221500	1.21665500	1.61180000	C	-4.35110900	0.75304700	-0.49870400
N	1.90164300	1.84849300	1.43850700	C	-5.30090600	1.63158300	0.03958200
H	2.18373300	2.46081000	2.18999700	C	-4.69042900	-0.59079400	-0.70892200
C	2.46840500	1.81612200	0.23980000	C	-6.58055900	1.18115300	0.33715900
Zr	-0.00280700	-0.02069500	0.01305600	H	-5.01838200	2.66304100	0.21300700
C	3.72602000	2.56352200	0.00002200	C	-5.97121700	-1.03764800	-0.39579800
C	4.63465200	2.85908700	1.02477400	H	-3.95883900	-1.30740200	-1.06449000
C	4.01176900	2.97136400	-1.30821000	C	-6.91842000	-0.15454600	0.11796400
C	5.79511300	3.57528500	0.74811800	H	-7.31446300	1.86941400	0.74291700
H	4.45864800	2.50107300	2.03439200	H	-6.22302400	-2.08180900	-0.54683800
C	5.17228300	3.68784000	-1.58000100	H	-7.91696900	-0.50754700	0.35471100
H	3.31253400	2.71729500	-2.09598000	H	-2.74265000	-0.00529600	-2.36979800
C	6.06439900	3.99532800	-0.55342500	C	-1.21789400	-3.44573800	1.13559600
H	6.49636300	3.79356900	1.54699200	C	-2.04934000	-4.53375600	1.42697900
H	5.38308100	4.00527700	-2.59608400	C	-0.36795300	-2.93365300	2.12527000
H	6.97147400	4.55111300	-0.76804100	C	-2.00845700	-5.12415100	2.68401800

C	-3.70175000	2.59370500	-0.09820400	H	-2.71711800	-4.90445500	0.65791300
C	-4.62160100	2.80909100	-1.13259300	C	-0.34215100	-3.52175700	3.38692900
C	-3.97804900	3.09169900	1.18052000	H	0.23191600	-2.05132300	1.93055000
C	-5.78417500	3.53647100	-0.89643700	C	-1.15338700	-4.62010500	3.66458500
H	-4.45349200	2.37717100	-2.11413800	H	-2.64570500	-5.97449300	2.90255000
C	-5.14026900	3.81956300	1.41148100	H	0.30416600	-3.11325700	4.15636700
H	-3.27077200	2.89743300	1.97815300	H	-1.12749100	-5.07767100	4.64820800
C	-6.04371000	4.04770300	0.37401700	H	0.73985200	-2.70626400	-0.36901800
H	-6.49502600	3.69131600	-1.70159900	C	1.29247300	3.98530900	1.24169200
H	-5.34383000	4.20774000	2.40425800	C	0.31380800	4.82073400	0.68762600
H	-6.95235300	4.61219700	0.55712600	C	2.32550100	4.54538500	2.00031100
C	-3.74654100	-2.55961700	0.12643800	C	0.36149300	6.19381000	0.91235600
C	-4.67595500	-2.75254700	1.15674000	H	-0.46690700	4.41619700	0.05180000
C	-4.02287100	-3.06249100	-1.15034500	C	2.36401500	5.91618700	2.22934100
C	-5.84867800	-3.46272500	0.91858500	H	3.09252200	3.89082300	2.39685200
H	-4.50634500	-2.31652200	2.13618900	C	1.38047900	6.74309000	1.68797100
C	-5.19540900	-3.77300700	-1.38325600	H	-0.39288700	6.83578200	0.46966000
H	-3.30720500	-2.88622500	-1.94467900	H	3.16508800	6.34133900	2.82525500
C	-6.10878600	-3.97878900	-0.34982100	H	1.41434000	7.81404400	1.86062600
H	-6.56673900	-3.60041600	1.72046100	H	-0.76665100	2.44386500	0.80341000
H	-5.39910000	-4.16531900	-2.37438100	H	2.70031300	0.72835600	-0.41496000
H	-7.02532600	-4.52984700	-0.53452100	C	3.31197200	-0.74274000	-1.79316000
C	3.70705200	-2.61442900	-0.03087900	C	4.21576600	-1.40745100	-0.79918400
C	4.10258500	-3.69487800	-0.83037700	C	4.18261800	-1.15678100	0.58102600
C	4.52708000	-2.21245400	1.02962700	C	5.13159300	-2.33788000	-1.30734200
C	5.31187400	-4.33983400	-0.59101900	C	5.05795600	-1.82996000	1.42964400
H	3.45331800	-4.06110800	-1.61941400	H	3.49289100	-0.43823500	1.01052500
C	5.73478900	-2.85976300	1.26639300	C	6.00231200	-3.00546400	-0.45545600
H	4.19830200	-1.39354800	1.65798900	H	5.14241800	-2.51966800	-2.37541700
C	6.13300400	-3.92103400	0.45459900	C	5.96672800	-2.75274900	0.91593000
H	5.60625600	-5.17957500	-1.21208800	H	5.03065600	-1.62719800	2.49510900
H	6.36615400	-2.53804300	2.08830600	H	6.71009300	-3.72170200	-0.85946700
H	7.07422800	-4.42757400	0.64245100	H	6.64799200	-3.27212800	1.58233600

trans-M(N,O_N), trans-Zr(ONHCPhO)$_4$			
O	0.56108800	-1.14554300	1.37097700
O	-0.38365000	2.12535000	0.00458700
O	-1.80050100	-0.71286500	-0.94632900
O	0.99563700	0.16309200	-1.89405200
N	-0.28579800	1.86120800	1.39183900

C	0.71161300	2.47103100	2.21569900
N	0.61980200	-2.21746300	0.45104000
C	-0.21566000	-3.35107000	0.55616700
N	2.04106900	0.57143300	-1.03013100
C	3.29393000	-0.11312200	-0.95688000
N	-2.34592500	-0.11299000	0.20684700
Zr	-0.07978300	0.09288600	-0.13000600
O	0.55878700	2.36459100	3.41148300
O	4.20808200	0.49902300	-0.44953100
O	0.09570800	-4.33227400	-0.08670300
O	-3.55408800	1.45535200	1.24963100
C	3.42003700	-1.53255000	-1.39786900
C	4.40338500	-2.29185600	-0.74183500
C	2.69485500	-2.10822200	-2.45192800
C	4.63030000	-3.61256400	-1.10595500
H	4.98031600	-1.82643100	0.04845700
C	2.94495200	-3.42653800	-2.82429400
H	1.94427400	-1.52839100	-2.96834900
C	3.90004100	-4.18223600	-2.14952200
H	5.37851000	-4.19670000	-0.58074500
H	2.38049400	-3.86668900	-3.63905900
H	4.07554100	-5.21441100	-2.43444900
H	2.20136700	1.57705700	-1.07956800
C	1.90117500	3.12373400	1.59811400
C	3.09968600	3.04345400	2.32026900
C	1.85654600	3.87765800	0.41576800
C	4.24639300	3.66931900	1.84883600
H	3.11561500	2.48288100	3.24737600
C	3.00475300	4.52389100	-0.03616300
H	0.93066600	3.96428000	-0.13527800
C	4.20106800	4.41080700	0.66947900
H	5.17564100	3.57992500	2.40102800
H	2.96240500	5.11791800	-0.94329600
H	5.09612000	4.90248200	0.30253700
H	-1.20022100	1.89251800	1.84559900
C	-1.48167000	-3.28745900	1.35267500
C	-1.61976100	-2.60077100	2.56795800
C	-2.55390600	-4.05217400	0.87051800
C	-2.82270300	-2.66713800	3.27129200
H	-0.79329100	-2.02587500	2.96109400

C	-3.75591300	-4.09732700	1.56582800				
H	-2.42504600	-4.60511000	-0.05212300				
C	-3.89343500	-3.40314100	2.76862300				
H	-2.91891400	-2.13964700	4.21433900				
H	-4.58408400	-4.67881600	1.17451300				
H	-4.83019400	-3.44164900	3.31509100				
H	1.57596500	-2.47968300	0.22437400				
H	-2.63047500	-0.79826800	0.90625500				
C	-3.22884500	1.01602800	0.16390000				
C	-3.65880100	1.61507800	-1.12324100				
C	-3.70694800	0.91936700	-2.33998800				
C	-4.12107800	2.93933600	-1.06537200				
C	-4.20704700	1.54909900	-3.47646400				
H	-3.35353500	-0.09981900	-2.39435000				
C	-4.60151400	3.56541100	-2.20643900				
H	-4.09725800	3.45888100	-0.11515900				
C	-4.64582400	2.86959500	-3.41552100				
H	-4.24882900	1.00497600	-4.41406600				
H	-4.94542700	4.59303400	-2.15537600				
H	-5.02463800	3.35713400	-4.30821300				
D-is2 (C_1 symmetry), $Zr_2(ONHCPhO)_8$				**D-is1 (C_2 symmetry), $Zr_2(ONHCPhO)_8$**			
O	-1.34444600	1.52435500	-1.34122000	O	-1.64220600	1.40107900	-0.74303900
O	-5.52360000	0.37492200	-1.10842200	O	-1.13497800	5.47646200	0.20488300
O	-4.57944400	1.13404000	1.24767000	O	1.03724300	4.51668900	-1.02763300
O	-1.61982200	-1.15337700	-1.49296800	O	-0.80485900	1.56473400	1.88477700
O	-4.01707300	-1.40888400	-0.00672900	O	0.38191700	4.07878600	1.77135400
N	-5.34252900	-1.62599600	-0.16603000	N	0.16659600	5.39379200	2.00213700
H	-5.70417900	-2.46230200	0.26713200	C	-0.61988700	6.07758500	1.18206700
C	-6.08214200	-0.69246700	-0.75390100	O	1.13497800	2.03004900	-0.20231300
O	-2.05993400	0.32471700	1.16627200	N	1.29245500	0.69417500	-0.06188100
N	-0.74641900	0.55691600	1.34462600	C	-1.70794900	0.15911900	-0.99502000
C	-0.08578400	1.65681100	-1.45964600	O	-2.48071200	3.40084400	1.07105300
O	-3.47055700	0.20321100	-2.70995100	N	-2.80080900	2.53382200	2.05093700
N	-2.56557300	-0.51690000	-3.40157500	C	-1.91625300	1.64996900	2.48748500
H	-2.61644600	-0.44578900	-4.40760800	O	-1.23167500	3.69734400	-1.90511900
C	-1.65604100	-1.22965300	-2.75039600	N	-0.55589000	4.66984900	-2.56178800
O	-3.70091400	2.53275500	-0.73144100	C	0.62992800	5.04202600	-2.09434400
N	-4.62637700	3.04121600	0.11622900	Zr	-0.59514300	3.20086500	0.07461400

H	-5.01081700	3.93811700	-0.13884400	O	1.64220600	-1.40107900	-0.74303900
C	-5.02700800	2.30018400	1.14506800	O	1.13497800	-5.47646200	0.20488300
Zr	-3.22145100	0.46598300	-0.61177900	O	-1.03724300	-4.51668900	-1.02763300
O	1.34640100	0.22662900	1.98636200	O	0.80485900	-1.56473400	1.88477700
O	5.45089100	-0.42216900	1.14343600	O	-0.38191700	-4.07878600	1.77135400
O	4.46423000	1.55027500	-0.40111200	N	-0.16659600	-5.39379200	2.00213700
O	1.58202500	-1.79649500	0.12565600	C	0.61988700	-6.07758500	1.18206700
O	4.12215800	-1.31726300	-0.88996400	O	-1.13497800	-2.03004900	-0.20231300
N	5.43310000	-1.60981500	-0.73231800	N	-1.29245500	-0.69417500	-0.06188100
H	5.87679200	-2.07035400	-1.51303300	C	1.70794900	-0.15911900	-0.99502000
C	6.08121300	-1.14042800	0.32592100	O	2.48071200	-3.40084400	1.07105300
O	2.03474100	0.70811500	-0.91115500	N	2.80080900	-2.53382200	2.05093700
N	0.69787200	0.63683200	-1.10305400	C	1.91625300	-1.64996900	2.48748500
C	0.12072400	-0.08233200	2.12497000	O	1.23167500	-3.69734400	-1.90511900
O	3.38746800	-1.81819100	1.98539200	N	0.55589000	-4.66984900	-2.56178800
N	2.53737800	-2.85375100	1.82626800	C	-0.62992800	-5.04202600	-2.09434400
H	2.70371800	-3.65611000	2.41593700	Zr	0.59514300	-3.20086500	0.07461400
C	1.62422700	-2.81953500	0.86916300	C	-1.43044300	-6.03913200	-2.84765000
O	3.61383100	1.42548000	2.02601500	C	-0.84843500	-6.97860400	-3.70847100
N	4.55601100	2.32698200	1.67341200	C	-2.81855900	-6.04401900	-2.66664800
H	4.92278600	2.89599000	2.42143300	C	-1.64608900	-7.88548200	-4.39961800
C	4.93378000	2.39552800	0.40398200	C	-3.61261900	-6.95058800	-3.36112800
Zr	3.17992000	-0.14507100	0.65052300	C	-3.02977300	-7.87008400	-4.23235300
H	0.24980000	-0.23891900	-0.83554300	C	0.88261600	-7.51113000	1.46161200
H	-0.35487000	1.31084700	0.79779600	C	2.11141000	-8.04833700	1.06069300
C	5.90240100	3.44141900	-0.00965600	C	-0.05657000	-8.33799000	2.09077300
C	6.00543400	4.67335000	0.64947800	C	2.40594200	-9.38387400	1.31285500
C	6.72260700	3.18626000	-1.11483300	C	0.24146700	-9.67478700	2.33886500
C	6.93405400	5.61993600	0.22735500	C	1.47446700	-10.19910600	1.95532200
H	5.33567200	4.91455000	1.46880400	C	2.29798100	-0.80578600	3.64947100
C	7.64996100	4.13438700	-1.53361700	C	1.79722200	0.49697400	3.75868500
H	6.61794600	2.24098300	-1.63387400	C	3.15059600	-1.29722100	4.64996500
C	7.76162500	5.35100400	-0.86144800	C	2.17593400	1.30180200	4.82888300
H	7.00039300	6.57432100	0.73945600	C	3.52094700	-0.48950600	5.71995300
H	8.28554800	3.92530400	-2.38800600	C	3.04001800	0.81588900	5.80790300
H	8.48288300	6.09163300	-1.19164900	C	-2.26218100	-0.28203100	-2.30142900
C	7.52070700	-1.46158800	0.49231000	C	-2.44183900	0.71729600	-3.27113000
C	8.32127200	-0.56873800	1.21375400	C	-2.64879100	-1.60019900	-2.58955900
C	8.09469800	-2.62908300	-0.02759800	C	-2.98487500	0.40028400	-4.51066600
C	9.67740700	-0.82425400	1.38507900	C	-3.20178700	-1.90344400	-3.83125400

H	7.86364900	0.31881900	1.63379500	C	-3.36668400	-0.91039000	-4.79471300
C	9.45191700	-2.88221300	0.14691900	C	2.26218100	0.28203100	-2.30142900
H	7.47769900	-3.36319500	-0.53615800	C	2.44183900	-0.71729600	-3.27113000
C	10.24734600	-1.97837300	0.84898700	C	2.64879100	1.60019900	-2.58955900
H	10.29105100	-0.12318600	1.94141900	C	2.98487500	-0.40028400	-4.51066600
H	9.88530100	-3.79343100	-0.25239600	C	3.20178700	1.90344400	-3.83125400
H	11.30484400	-2.17884600	0.98765200	C	3.36668400	0.91039000	-4.79471300
C	0.72817900	-3.99344900	0.72401700	C	1.43044300	6.03913200	-2.84765000
C	0.33790600	-4.40415200	-0.55408200	C	0.84843500	6.97860400	-3.70847100
C	0.26866300	-4.69823900	1.84458500	C	2.81855900	6.04401900	-2.66664800
C	-0.47268200	-5.52316700	-0.71119100	C	1.64608900	7.88548200	-4.39961800
H	0.67269500	-3.84379600	-1.41653600	C	3.61261900	6.95058800	-3.36112800
C	-0.54516100	-5.81537400	1.68207100	C	3.02977300	7.87008400	-4.23235300
H	0.50073900	-4.34628000	2.84411000	C	-0.88261600	7.51113000	1.46161200
C	-0.91162200	-6.23449300	0.40466300	C	0.05657000	8.33799000	2.09077300
H	-0.76653500	-5.83536300	-1.70788900	C	-2.11141000	8.04833700	1.06069300
H	-0.90765400	-6.34672500	2.55607000	C	-0.24146700	9.67478700	2.33886500
H	-1.54877900	-7.10443900	0.27979200	C	-2.40594200	9.38387400	1.31285500
C	0.44825500	2.94874400	-1.96684300	C	-1.47446700	10.19910600	1.95532200
C	-0.49187500	3.97615600	-2.15345000	C	-2.29798100	0.80578600	3.64947100
C	1.79530700	3.18151600	-2.28891800	C	-3.15059600	1.29722100	4.64996500
C	-0.09376400	5.21054900	-2.65158500	C	-1.79722200	-0.49697400	3.75868500
H	-1.52817500	3.78164100	-1.90387400	C	-3.52094700	0.48950600	5.71995300
C	2.18069700	4.42153200	-2.79274800	C	-2.17593400	-1.30180200	4.82888300
H	2.52888700	2.40449600	-2.13193200	C	-3.04001800	-0.81588900	5.80790300
C	1.24423500	5.43689100	-2.97377400	H	0.23047900	-7.03276600	-3.81318100
H	-0.82883700	5.99715900	-2.79078100	H	-3.25626200	-5.33328000	-1.97578000
H	3.22373900	4.59251200	-3.03920200	H	-1.18523900	-8.61447100	-5.05818400
H	1.55532600	6.40182100	-3.36305100	H	-4.68847000	-6.94246200	-3.21931200
C	-0.30709800	-1.04764800	3.17015000	H	-3.64997400	-8.57976000	-4.77037800
C	0.65664200	-1.39012800	4.13287700	H	2.82116700	-7.40357900	0.55581900
C	-1.59590700	-1.59652200	3.26236200	H	-1.03684900	-7.95199100	2.35242300
C	0.33655000	-2.25341400	5.17383800	H	3.36372000	-9.79124800	1.00552100
H	1.64967200	-0.96719900	4.04595600	H	-0.49555200	-10.31075700	2.81839800
C	-1.90241800	-2.46958900	4.30415100	H	1.70431900	-11.24229800	2.14702100
H	-2.34205300	-1.34321400	2.52358700	H	1.10797500	0.88636900	3.02002000
C	-0.94619000	-2.79685300	5.26262800	H	3.49692300	-2.32538600	4.61713800
H	1.08625200	-2.49775400	5.92020700	H	1.78837500	2.31299900	4.89076000
H	-2.90027200	-2.89226000	4.36541900	H	4.17454800	-0.88403600	6.49126100
H	-1.19799900	-3.46930900	6.07747100	H	3.32955200	1.44651900	6.64252000

C	-5.99307700	2.87987600	2.11315300	H	-2.15398800	1.73352100	-3.02831300
C	-6.06836600	4.25586000	2.36450000	H	-2.51008800	-2.37294700	-1.84736200
C	-6.83815600	2.00964500	2.81069600	H	-3.11444200	1.17845600	-5.25651900
C	-6.99427100	4.75328500	3.27663400	H	-3.50218700	-2.92428100	-4.04604600
H	-5.37884900	4.93953800	1.87959300	H	-3.79336700	-1.15639900	-5.76263300
C	-7.76314800	2.51004200	3.72055700	H	2.15398800	-1.73352100	-3.02831300
H	-6.75394400	0.94483600	2.62982700	H	2.51008800	2.37294700	-1.84736200
C	-7.84699700	3.88243200	3.95253100	H	3.11444200	-1.17845600	-5.25651900
H	-7.03876200	5.81988200	3.47132500	H	3.50218700	2.92428100	-4.04604600
H	-8.41755400	1.82793100	4.25354600	H	3.79336700	1.15639900	-5.76263300
H	-8.56575300	4.27119400	4.66669600	H	-0.23047900	7.03276600	-3.81318100
C	-7.53285800	-0.93988100	-0.95021700	H	3.25626200	5.33328000	-1.97578000
C	-8.06197200	-2.22921500	-1.09268300	H	1.18523900	8.61447100	-5.05818400
C	-8.39189200	0.16297600	-1.01443900	H	4.68847000	6.94246200	-3.21931200
C	-9.43061300	-2.41123100	-1.26670600	H	3.64997400	8.57976000	-4.77037800
H	-7.40460100	-3.09284300	-1.10688300	H	1.03684900	7.95199100	2.35242300
C	-9.75921900	-0.02265300	-1.18717500	H	-2.82116700	7.40357900	0.55581900
H	-7.97080300	1.15740400	-0.92877100	H	0.49555200	10.31075700	2.81839800
C	-10.28278400	-1.30917700	-1.30924200	H	3.36372000	9.79124800	1.00552100
H	-9.82986100	-3.41341900	-1.38415300	H	-1.70431900	11.24229800	2.14702100
H	-10.41803100	0.83853100	-1.23021300	H	-3.49692300	2.32538600	4.61713800
H	-11.34948600	-1.45229400	-1.44849800	H	-1.10797500	-0.88636900	3.02002000
C	-0.74179700	-2.05897200	-3.58602500	H	-4.17454800	0.88403600	6.49126100
C	-1.25918200	-2.83004600	-4.63602100	H	-1.78837500	-2.31299900	4.89076000
C	0.63785800	-2.06700400	-3.34704500	H	-3.32955200	-1.44651900	6.64252000
C	-0.41095300	-3.58698300	-5.44057200	H	0.53859200	5.75459800	2.86809400
H	-2.33097300	-2.86200100	-4.80422100	H	-3.74551200	2.59988100	2.40093200
C	1.48190000	-2.81834800	-4.15964500	H	0.98753100	0.29377500	0.81907400
H	1.06000000	-1.48700900	-2.53756500	H	-0.53859200	-5.75459800	2.86809400
C	0.96242900	-3.57869600	-5.20679000	H	3.74551200	-2.59988100	2.40093200
H	-0.82472100	-4.18780800	-6.24414800	H	0.91111500	-4.90371300	-3.47666200
H	2.54906900	-2.80465300	-3.96533600	H	-0.98753100	-0.29377500	0.81907400
H	1.62475300	-4.16575200	-5.83511800	H	-0.91111500	4.90371300	-3.47666200

H-substitution model, $Zr(ONHCHO)_4$				**Methyl-substitution model, $Zr(ONHCMeO)_4$**			
O	1.93226300	-1.15246000	0.71876900	O	1.91717400	-1.17514100	0.68945300
O	-1.93012400	1.15391100	0.71989200	O	-1.91675600	1.17565500	0.68968100
O	-1.93247700	-1.15239800	-0.71892900	O	-1.91688100	-1.17516500	-0.68929900
O	1.93070200	1.15371200	-0.72015200	O	1.91634100	1.17574200	-0.68955300

O -0.68692600 1.28731500 -1.55402400	O -0.69049600 1.26638600 -1.57229100
N -1.88538600 1.89052300 -1.38040600	N -1.88674700 1.87664800 -1.41034500
H -2.24807900 2.40551200 -2.17015100	H -2.23721200 2.37946500 -2.21247500
C -2.46317400 1.81246600 -0.19978900	C -2.47335300 1.83017100 -0.22645900
O 0.68532400 -1.28859700 -1.55307100	O 0.69013700 -1.26660700 -1.57207400
N 1.88419200 -1.89143200 -1.38067800	N 1.88626400 -1.87712200 -1.41022800
H 2.24560900 -2.40739400 -2.17036500	H 2.23626900 -2.38051900 -2.21219600
C 2.46381500 -1.81194000 -0.20101200	C 2.47334400 -1.83013800 -0.22659200
O 0.68724900 1.28728200 1.55380700	O 0.69027000 1.26640600 1.57244400
N 1.88617200 1.88969200 1.38042600	N 1.88628400 1.87706100 1.41033000
H 2.24892400 2.40463400 2.17017100	H 2.23680500 2.37981900 2.21247600
C 2.46393300 1.81170600 0.19977400	C 2.47292800 1.83046800 0.22648600
O -0.68597600 -1.28799700 1.55334900	O -0.68982600 -1.26673900 1.57214300
N -1.88496600 -1.89059200 1.38084300	N -1.88587100 -1.87743300 1.41025600
H -2.24668500 -2.40622000 2.17060900	H -2.23594000 -2.38068600 2.21228700
C -2.46433000 -1.81137800 0.20102700	C -2.47296200 -1.83042800 0.22663800
Zr -0.00005000 0.00009600 0.00002300	Zr -0.00000800 0.00011200 -0.00002500
H 3.41274400 -2.34361500 -0.07969200	C -3.77012200 2.56179800 -0.02250400
H 3.41290300 2.34313000 0.07773700	H -4.11167600 3.07974500 -0.92142000
H -3.41340100 -2.34282800 0.07977700	H -4.54235900 1.85594300 0.29131700
H -3.41182800 2.34434900 -0.07743900	H -3.64830900 3.29223500 0.78052700
	C -3.76949200 -2.56244600 0.02263600
	H -3.64759300 -3.29237300 -0.78084700
	H -4.11057600 -3.08104400 0.92135500
	H -4.54211900 -1.85674300 -0.29056300
	C 3.77016900 -2.56172800 -0.02283200
	H 4.11076200 -3.08104200 -0.92132500
	H 4.54286000 -1.85553500 0.28915200
	H 3.64903700 -3.29092400 0.78141100
	C 3.76957000 2.56223100 0.02233100
	H 3.64776400 3.29209600 -0.78121300
	H 4.11082200 3.08082700 0.92098700
	H 4.54205200 1.85634800 -0.29084800
H-substitution model, $Zr_2(ONHCHO)_8$	**Methyl-substitution model, $Zr_2(ONHCMeO)_8$**
O 1.34783900 1.54636300 -0.51015300	O 1.53969900 0.02319100 -1.54278300
O 0.55641900 5.52682700 0.67841800	O 5.65169700 -0.26793700 -0.55031000
O -1.11446100 3.90425100 2.03534900	O 4.21859400 -1.70994400 1.22580700
O -0.57119600 2.52117100 -2.14216800	O 2.14476700 2.10515300 0.06569000

O	-1.51731800	4.69623100	-0.68759100	O	4.48249200	1.16079300	1.27529600
N	-1.36368000	5.99921000	-0.35765900	N	5.82980500	1.14421200	1.15269200
C	-0.29871900	6.36900100	0.32116400	C	6.39047900	0.40982800	0.20785200
O	-1.39695000	1.83080000	0.39730700	O	1.91959400	-0.40981100	1.31230000
N	-1.51731800	0.70397900	-0.35795500	N	0.68591300	0.15508100	1.37455100
C	1.42386300	0.49502500	0.17630300	C	0.41145600	-0.54362100	-1.62022900
O	1.36081600	4.15061400	-1.44782400	O	3.94733700	1.38291100	-1.69001200
N	1.28098900	3.63582500	-2.69440700	N	3.21207200	2.50589200	-1.84438200
C	0.28403100	2.83848000	-3.00365600	C	2.32511800	2.85401100	-0.93059900
O	1.29994900	2.99816400	1.67326000	O	3.44163700	-1.82445800	-1.23196100
N	0.89415700	3.44907800	2.88762400	N	4.13885000	-2.84676800	-0.67452600
C	-0.34742700	3.87352400	3.01864800	C	4.49423200	-2.75837600	0.59806000
Zr	0.00114200	3.35802600	0.01343200	Zr	3.36817200	0.01854300	-0.14899500
O	-1.34783900	-1.54636300	-0.51015300	O	-1.54034700	0.02390300	1.54344700
O	-0.55641900	-5.52682700	0.67841800	O	-5.65097500	-0.26839200	0.55260800
O	1.11446100	-3.90425100	2.03534900	O	-4.22037800	-1.70801400	-1.22736300
O	0.57119600	-2.52117100	-2.14216800	O	-2.14496600	2.10492600	-0.06745600
O	1.51731800	-4.69623100	-0.68759100	O	-4.48396000	1.16124300	-1.27407900
N	1.36368000	-5.99921000	-0.35765900	N	-5.83114400	1.14347800	-1.15052700
C	0.29871900	-6.36900100	0.32116400	C	-6.39064600	0.40885600	-0.20517900
O	1.39695000	-1.83080000	0.39730700	O	-1.92023100	-0.41027900	-1.31276900
N	1.51731800	-0.70397900	-0.35795500	N	-0.68674800	0.15497500	-1.37644900
C	-1.42386300	-0.49502500	0.17630300	C	-0.41199900	-0.54259300	1.62227400
O	-1.36081600	-4.15061400	-1.44782400	O	-3.94672800	1.38406300	1.68967400
N	-1.28098900	-3.63582500	-2.69440700	N	-3.21123500	2.50704700	1.84291700
C	-0.28403100	-2.83848000	-3.00365600	C	-2.32468600	2.85444800	0.92848700
O	-1.29994900	-2.99816400	1.67326000	O	-3.43931400	-1.82571200	1.22922500
N	-0.89415700	-3.44907800	2.88762400	N	-4.13676800	-2.84761500	0.67121800
C	0.34742700	-3.87352400	3.01864800	C	-4.49426300	-2.75750700	-0.60067100
Zr	-0.00114200	-3.35802600	0.01343200	Zr	-3.36809100	0.01890800	0.14896600
H	-2.09517500	6.62769700	-0.65924000	H	6.33845000	1.70713800	1.81878800
H	-2.00106700	-3.92059500	-3.34390600	H	3.40604800	3.04363500	-2.67666900
H	-1.57493900	-3.40906600	3.63250900	H	0.63763400	1.12614900	1.08064400
H	1.46978000	-0.84874400	-1.36335000	H	-6.34075600	1.70617400	-1.81608200
H	1.57493900	3.40906600	3.63250900	H	-3.40467200	3.04536100	2.67496100
H	-0.20899800	7.43489200	0.55170600	H	-4.32783900	-3.63375300	1.27435600
H	-0.65332400	4.18966500	4.02136500	H	-0.63903100	1.12706900	-1.08589900
H	0.24636900	2.47728300	-4.03546800	H	4.33140300	-3.63183300	-1.27859500
H	1.39833100	0.51557100	1.26837200	C	-7.88731000	0.41332500	-0.06768300
H	-1.39833100	-0.51557100	1.26837200	H	-8.15497400	0.76994500	0.92945100

H -0.24636900 -2.47728300 -4.03546800	H -8.38125700 1.04229500 -0.81155300
H 0.65332400 -4.18966500 4.02136500	H -8.26516200 -0.60707500 -0.16371000
H 0.20899800 -7.43489200 0.55170600	C -1.56306200 4.13528000 1.12751800
	H -1.88563900 4.68500200 2.01420000
	H -0.49707000 3.91719600 1.22354000
	H -1.69654100 4.77558400 0.25266000
	C -5.20637400 -3.91721200 -1.23936800
	H -5.36178400 -4.75226800 -0.55265900
	H -6.17621900 -3.58465900 -1.61557300
	H -4.62527400 -4.26797100 -2.09505400
	C -0.24947600 -1.98526300 2.00976000
	H 0.34753700 -2.51885800 1.26742400
	H 0.29683900 -2.05735300 2.95396700
	H -1.23691200 -2.42914700 2.10451700
	C 0.24903300 -1.98816300 -2.00080200
	H -0.33764900 -2.52058100 -1.24930100
	H -0.30790700 -2.06595400 -2.93821900
	H 1.23668700 -2.42967200 -2.10396400
	C 5.20608700 -3.91851400 1.23621900
	H 4.62410400 -4.27053400 2.09077700
	H 5.36264700 -4.75266800 0.54867600
	H 6.17535800 -3.58603400 1.61398800
	C 7.88722100 0.41531300 0.07130400
	H 8.15528400 0.77238400 -0.92555800
	H 8.38025900 1.04442400 0.81566000
	H 8.26568700 -0.60485800 0.16730900
	C 1.56396700 4.13495800 -1.13076500
	H 1.88682700 4.68384800 -2.01785900
	H 0.49790300 3.91720900 -1.22669500
	H 1.69759100 4.77592200 -0.25640800

5. Competing synthesis of SUM-1(Zr) vs UiO-66(Zr)

As a benchmark Zr-MOF, UiO-66 was originally synthesized by straightforward solvothermal reaction between $ZrCl_4$ and terephthalic acid (H_2-BDC),[13] similar to the synthetic procedure for SUM-1(Zr) as described in Section 2.2. To reveal the reactivity preference (if any) of $ZrCl_4$ when both H_2-BDC and H_2-BDHA are present, the following experiments were carried out.

Powders of $ZrCl_4$ (0.014 g, 6×10^{-5} mol), H_2-BDHA (0.039 g, 2×10^{-4} mol), **and** H_2-BDC (0.010 g, 6×10^{-5} mol) were mixed with DMF (2 mL) in a 4-mL glass vial before tightly capped and briefly sonicated. The mixture was heated in a 120 ºC isothermal oven for various periods of time (2 hours, 24 hours). After corresponding reaction time periods, all the solids were collected for PXRD characterization. As shown in Fig. S16, no peak corresponding of UiO-66 was observed, only SUM-1(Zr) was present. The outcome of this competing synthesis demonstrates a reactivity preference of $ZrCl_4$ with H_2-BDHA over H_2-BDC, in terms of MOF formation.

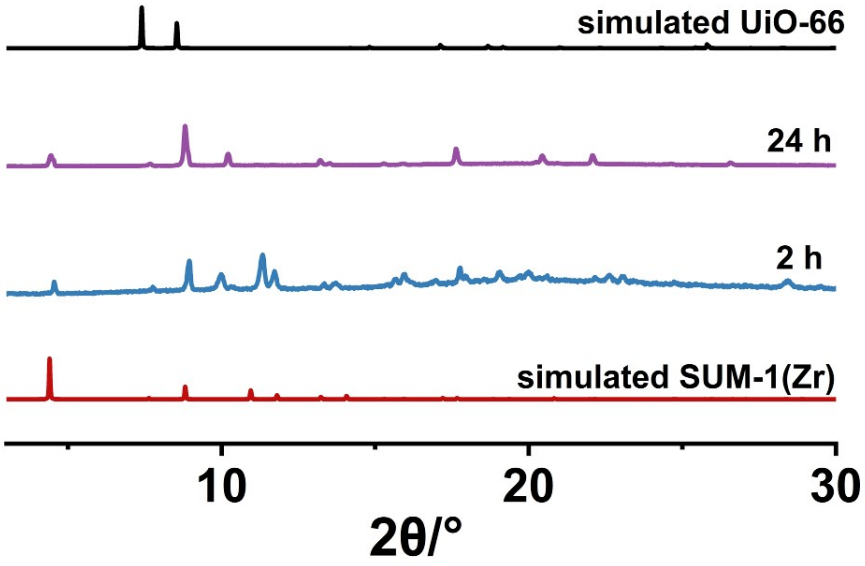

Fig. S16 Comparison of the experimental PXRD patterns of the as-synthesized products after different reaction time periods (2 h, blue; 24 h, purple) from the competing synthesis of H_2-BDHA against H_2-BDC with $ZrCl_4$, to the simulated patterns of SUM-1(Zr) (red) and UiO-66 (black).

As control experiments, $ZrCl_4$ (0.014 g, 6×10^{-5} mol) was reacted with H_2-BDHA (0.039 g, 2×10^{-4} mol) **or** H_2-BDC (0.010 g, 6×10^{-5} mol) in DMF (2 mL) in 4-mL glass vials, respectively, before tightly capped and sonicated. The conditions are otherwise the same comparing to the competing synthesis, except in the absence of the competing MOF ligand. The mixtures were heated in a 120 ºC isothermal oven. As shown in Fig. S17, after 2 h, crystals corresponding to SUM-1(Zr) and UiO-66 formed, respectively. We note that after 40 min, SUM-1(Zr) crystals were already present, while the $ZrCl_4$/H_2-BDC reaction mixture was still clear. These results confirm the amounts of reagents used in the aforementioned competing synthesis could indeed form SUM-1(Zr) and UiO-66 separately. When mixed together, however, the formation of SUM-1(Zr) dominated over UiO-66.

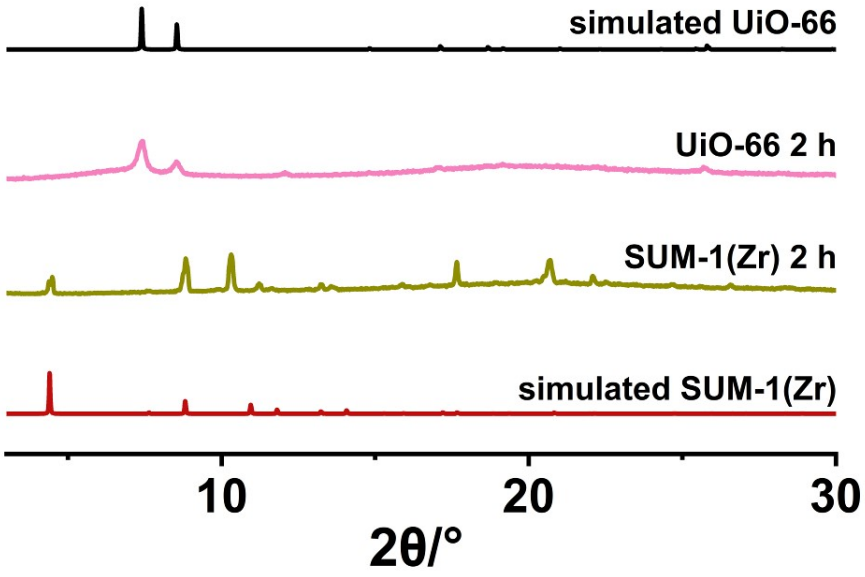

Fig. S17 Comparison of the experimental PXRD patterns of as-synthesized SUM-1(Zr) after 2 h (dark yellow) and UiO-66 after 2 h (pink) from conditions absent of the competing ligand, to the simulated patterns of SUM-1(Zr) (red) and UiO-66 (black).

In addition, according to literature,[14,15] formation of UiO-66 could be accelerated (autocatalyzed) by HCl. To study if the "expedited" UiO-66 crystallization could compete with the formation of SUM-1(Zr), the following experiments were carried out.

Powders of $ZrCl_4$ (0.014 g, 6×10^{-5} mol), H_2-BDHA (0.039 g, 2×10^{-4} mol), **and** H_2-BDC (0.010 g, 6×10^{-5} mol) were mixed with DMF (2 mL) and HCl/H_2O (0.050 mL, 37%) in a 4-mL glass vial before tightly capped and sonicated. The mixture was heated in a 120 ºC isothermal oven for various periods of time (20 minutes, 2 hours, 24 hours). After corresponding reaction time periods, all the solids were collected for PXRD characterization. As shown in Fig. S18, no peak corresponding of UiO-66 was observed in the presence of HCl for any of the tested samples, while SUM-1(Zr) were present in all cases. The outcome of this competing synthesis demonstrates a reactivity preference of $ZrCl_4$ with H_2-BDHA over H_2-BDC in terms of MOF formation, while accelerated in the presence of HCl.

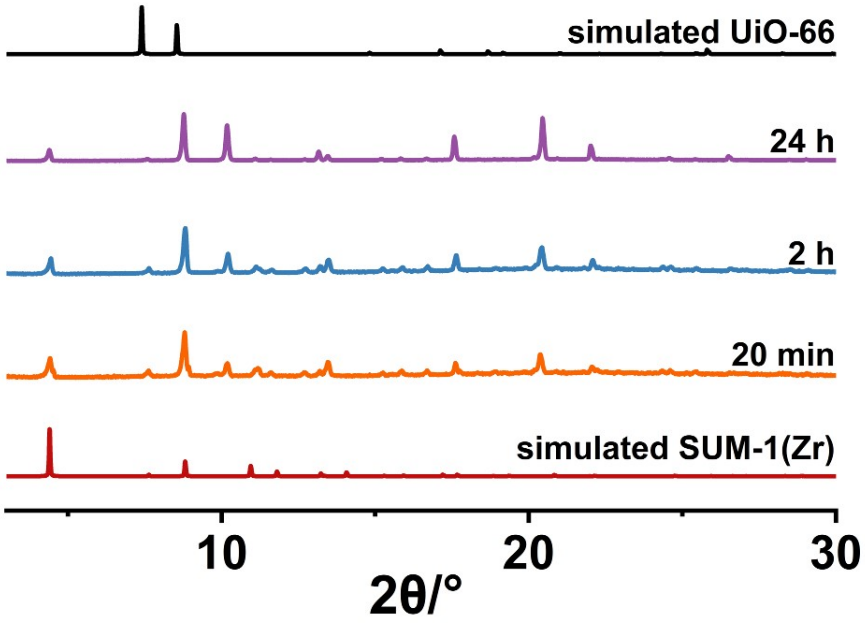

Fig. S18 Comparison of the experimental PXRD patterns of the as-synthesized products after different reaction time periods (20 min, orange; 2 h, blue; 24 h, purple) from the competing synthesis of H_2-BDHA against H_2-BDC with $ZrCl_4$, in the presence of HCl, to the simulated patterns of SUM-1(Zr) (red) and UiO-66 (black).

As control experiments, $ZrCl_4$ (0.014 g, 6×10^{-5} mol) was also reacted with H_2-BDHA (0.039 g, 2×10^{-4} mol) **or** H_2-BDC (0.010 g, 6×10^{-5} mol) in DMF (2 mL) and HCl/H_2O (0.050 mL, 37%) in 4-mL glass vials, respectively, before tightly capped and sonicated. The conditions are otherwise the same comparing to the competing synthesis (with HCl added), except in the absence of the competing MOF ligand. The mixtures were heated in a 120 ºC isothermal oven. As shown in Fig. S19, after 20 min, crystals corresponding to SUM-1(Zr) were already present, while after 40 min, crystals of UiO-66 formed. We also note that after 20 min, the solution of $ZrCl_4$ and H_2-BDC was still clear, without solids that could be separated for PXRD characterization. These results confirm: 1) HCl could indeed accelerate the formation of MOFs in both cases under these specific conditions; 2) the amounts of reagents used in the aforementioned competing synthesis could form SUM-1(Zr) and UiO-66 separately. When mixed together, however, the formation of SUM-1(Zr) dominated over UiO-66, even in the presence of HCl.

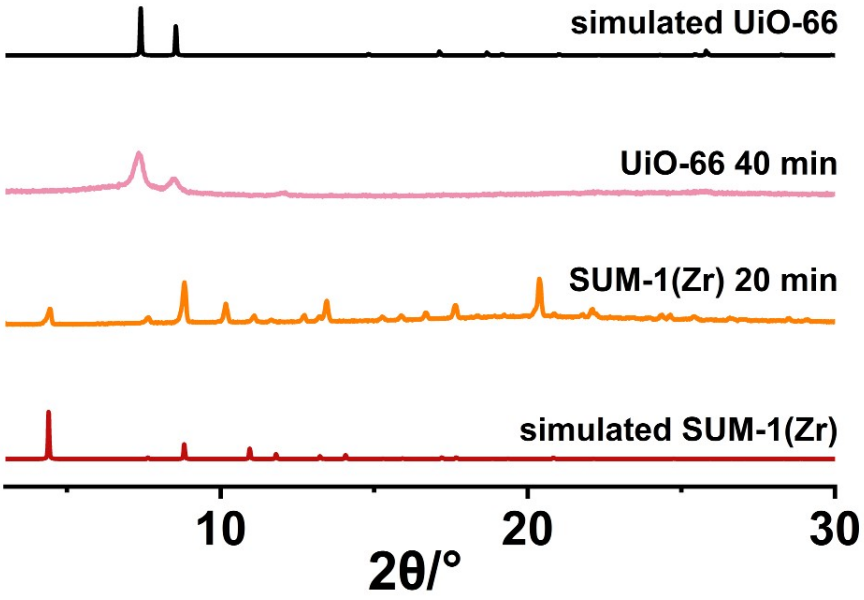

Fig. S19 Comparison of the experimental PXRD patterns of as-synthesized SUM-1(Zr) after 20 min (orange) and UiO-66 after 40 min (pink) from HCl-accelerated conditions absent of the competing ligand, to the simulated patterns of SUM-1(Zr) (red) and UiO-66 (black).

6. Characterization and stability study of SUM-1(Zr) and SUM-1(Hf)

6.1 PXRD of as-synthesized SUM-1(Zr) and SUM-1(Hf)

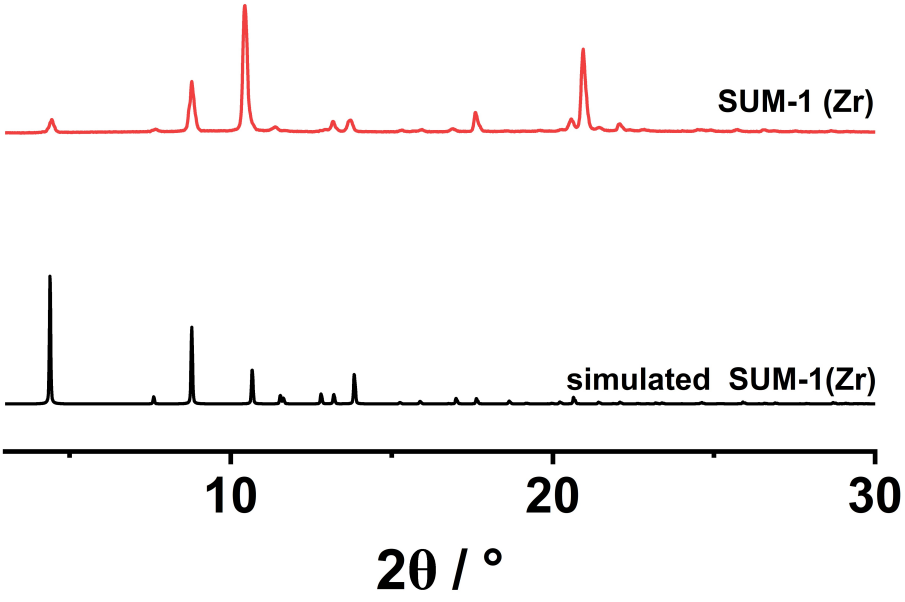

Fig. S20 Comparison of the experimental PXRD pattern of as-synthesized (red) SUM-1(Zr) to the simulated (black) pattern.

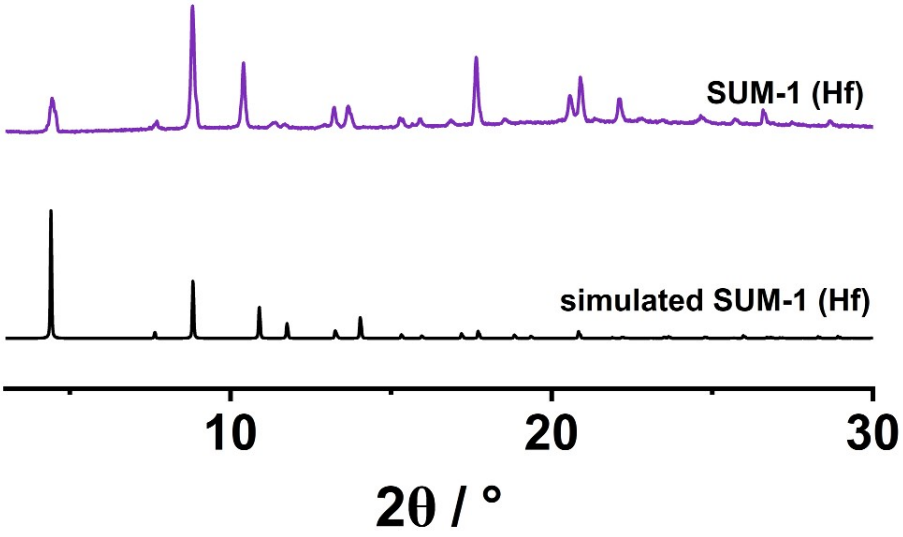

Fig. S21 Comparison of the experimental PXRD pattern of as-synthesized (purple) SUM-1(Hf) to the simulated (black) pattern.

6.2 FTIR of SUM-1(Zr) and SUM-1(Hf)

For FTIR, the as-synthesized MOFs were washed with dry DMF (3X), exchanged with DCM (3X), soaked in DCM at room temperature overnight and dried in air. The MOF samples (~1 mg) were mixed and crushed with KBr (~100 mg) and compressed to make pellets before collection of the corresponding FTIR spectra in the range of 400-4000 cm^{-1}. Zoomed-in spectra in the range of 500-2000 cm^{-1} are shown in Fig. S22.

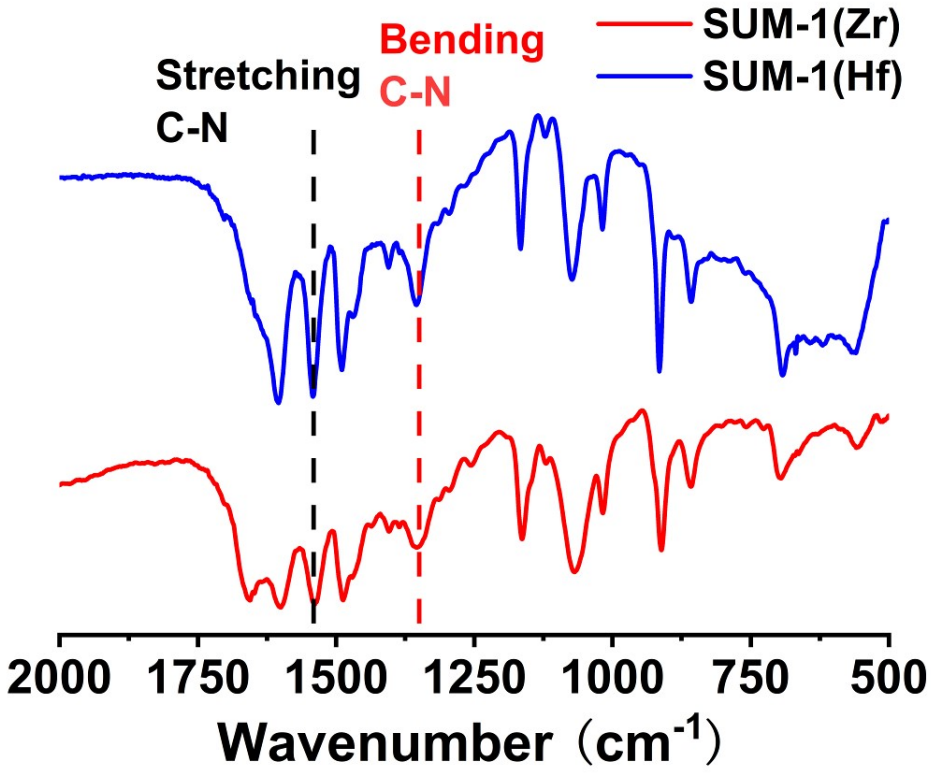

Fig. S22 FTIR spectra of SUM-1(Zr) (red) and SUM-1(Hf) (blue).[16]

6.3 Thermogravimetric analysis (TGA) of SUM-1(Zr) and SUM-1(Hf)

For TGA, the as-synthesized MOF crystals were washed with dry DMF (3X), DCM (3X) and dried with N_2 flow until they became free-flowing solids, and then loaded into a ceramic pan for analysis.

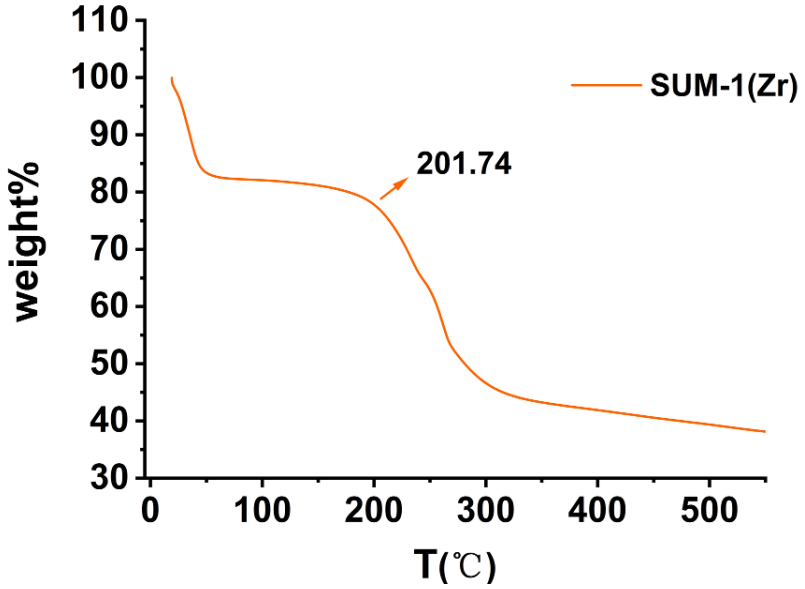

Fig. S23 TGA profile of SUM-1(Zr).

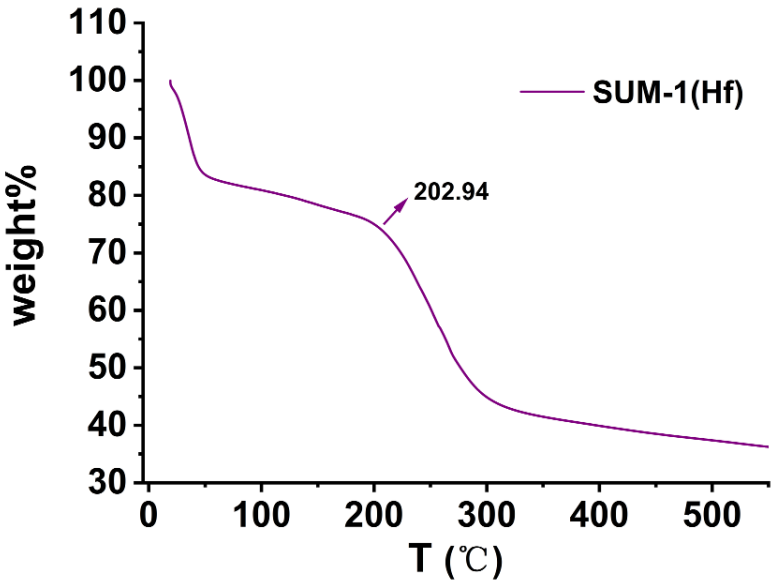

Fig. S24 TGA profile of SUM-1(Hf).

6.4 N_2 sorption of pristine SUM-1(Zr) and SUM-1(Hf)

The same activation procedure was performed on both SUM-1(Zr) and SUM-1(Hf): as-synthesized MOFs were washed with dry DMF (3X) and exchanged with acetone (3X) for 72 hours, followed by activation at 100 ºC for 12 hours on the degas station of BELSORP MAX. After N_2 adsorption-desorption isotherms (Fig. S25-S26) were acquired at 77 K, Brunauer-Emmett-Teller (BET) surface area was calculated, as summarized in Fig. S27-S28, Tables S7-S8. Pore size distribution was estimated using the non-local density functional theory (NLDFT) for the adsorption data points using a cylindrical pore metal oxide model, as shown in Fig. S29-S30.

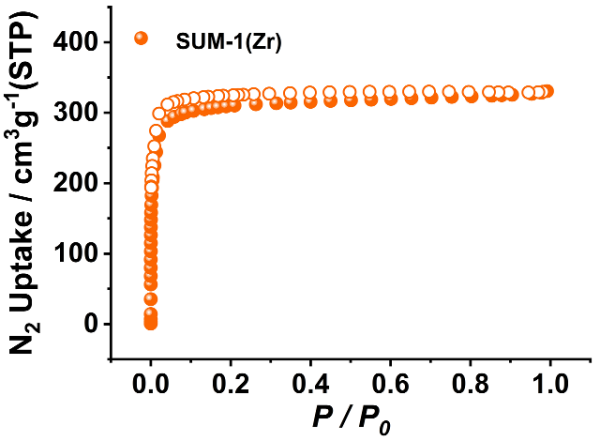

Fig. S25 N_2 adsorption-desorption isotherms of SUM-1(Zr) at 77 K (adsorption: filled circles; desorption: open circles).

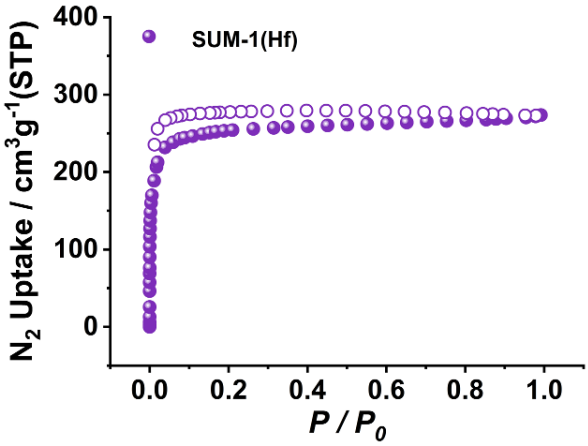

Fig. S26 N_2 adsorption-desorption isotherms of SUM-1(Hf) at 77 K (adsorption: filled circles; desorption: open circles).

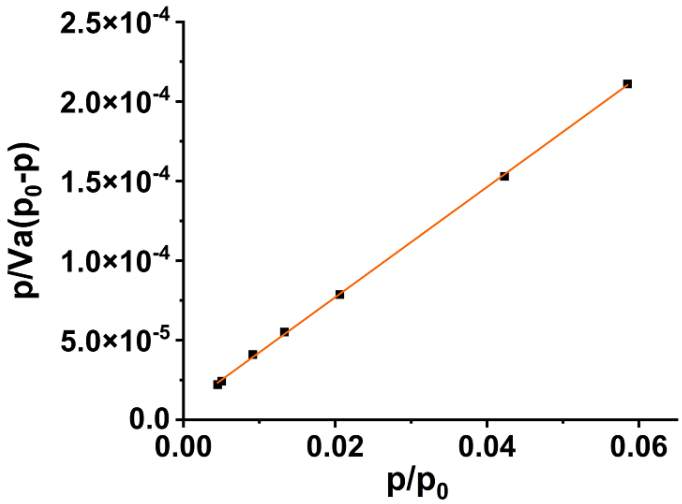

Fig. S27 Multi-point BET plot of SUM-1(Zr).

Table S7 Parameters for SUM-1(Zr) calculated from BET analysis

BET Area (m^2g^{-1})	**1252.5**
Slope	**3.4701×10^{-3}**
Intercept	**7.6415×10^{-6}**
R^2	**0.99972**
C	**455.12**
V_m [cm^3(STP)g^{-1}]	**287.54**

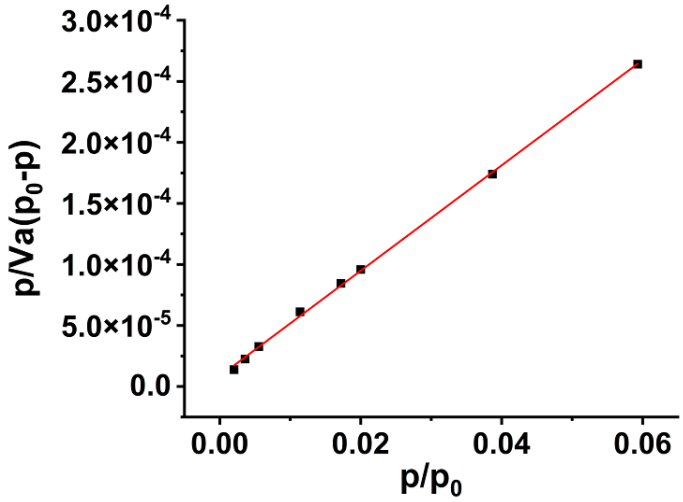

Fig. S28 Multi-point BET plot of SUM-1(Hf).

Table S8 Parameters for SUM-1(Hf) calculated from BET analysis

BET Area (m^2g^{-1})	**1005.5**
Slope	**4.3202×10^{-3}**
Intercept	**8.4480×10^{-6}**
R^2	**0.99935**
C	**512.39**
Vm [cm^3(STP)g^{-1}]	**231.02**

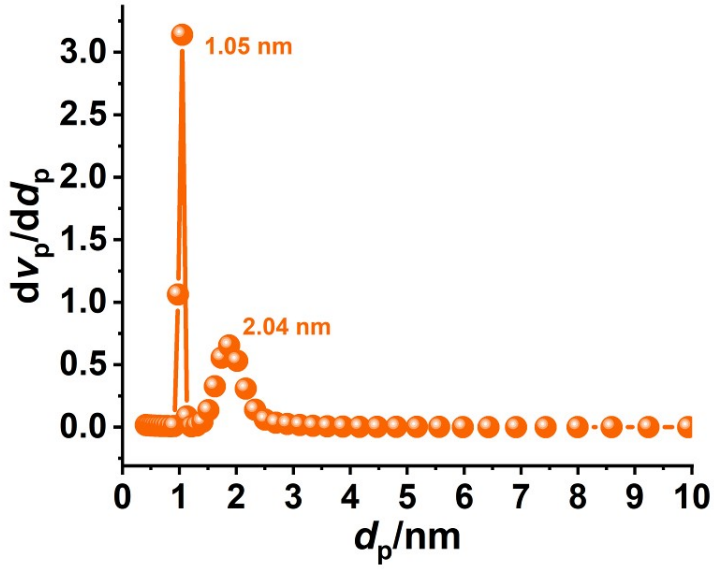

Fig. S29 Pore size distribution plot of SUM-1(Zr).

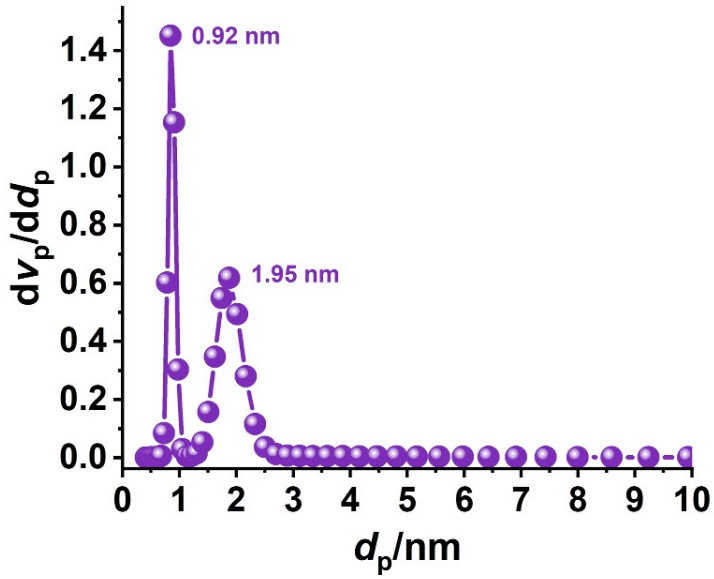

Fig. S30 Pore size distribution plot of SUM-1(Hf).

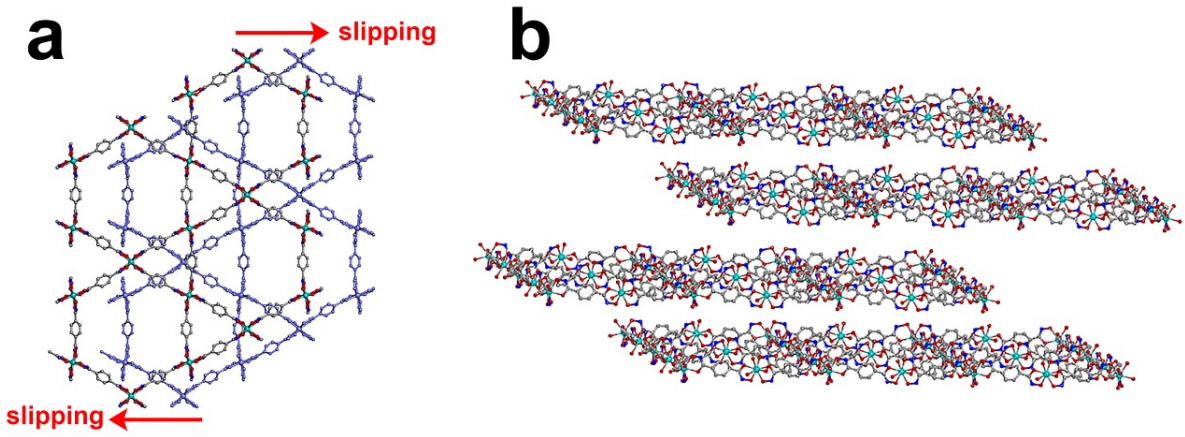

Fig. S31 Illustration of the proposed interlayer translation phenomenon, using a SUM-1(Zr) structure model, shown in (a): top view, (b) side view.

6.5 Stability of SUM-1(Zr) and SUM-1(Hf) in aqueous solutions with varied pH

For SUM-1(Zr) and SUM-1(Hf), as-synthesized MOFs were washed with dry DMF (3X), then washed (3X) and soaked (24 hours) in aqueous solutions with corresponding pH values. Solutions with different pH were obtained by adding HCl or NaOH. After 24 hours, the samples were examined with PXRD. The results are summarized in Fig. S32 and S33.

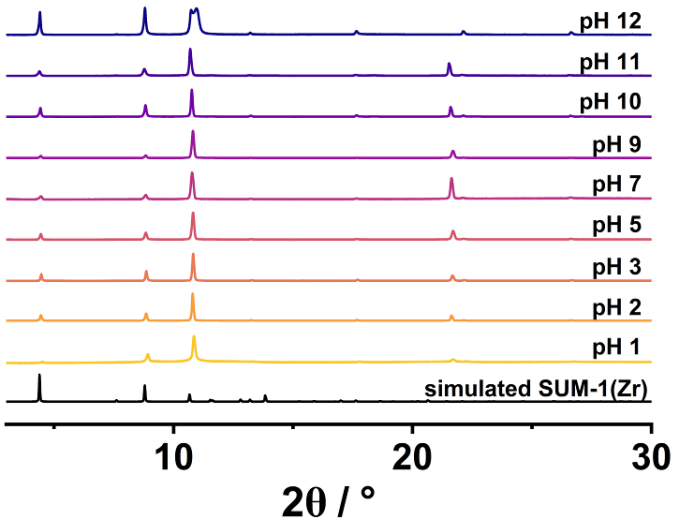

Fig. S32 PXRD patterns of SUM-1(Zr) after exposure to aqueous solutions of different pH for 24 hours, comparing to the simulated pattern.

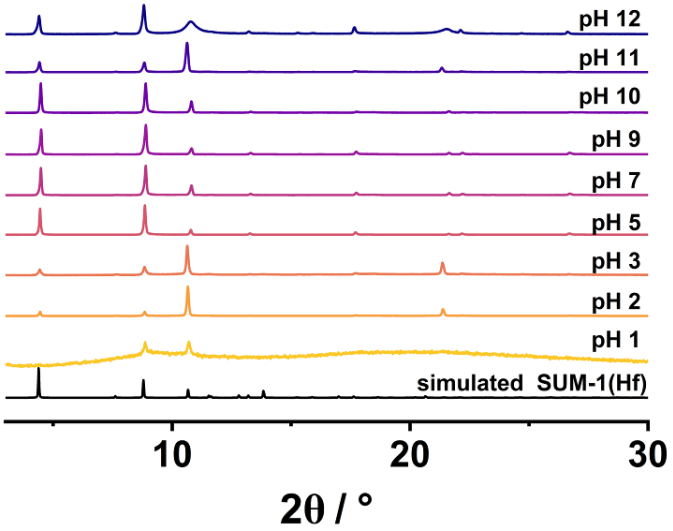

Fig. S33 PXRD patterns of SUM-1(Hf) after exposure to aqueous solutions of different pH for 24 hours, comparing to the simulated pattern.

6.6 Stability of SUM-1(Zr) and SUM-1(Hf) in various organic solvents

For SUM-1(Zr) and SUM-1(Hf), as-synthesized MOFs were washed with dry DMF (3X), then washed (3X) and soaked (24 hours) in various organic solvents. After 24 hours, the samples were examined with PXRD. The results are summarized in Fig. S34 and S35.

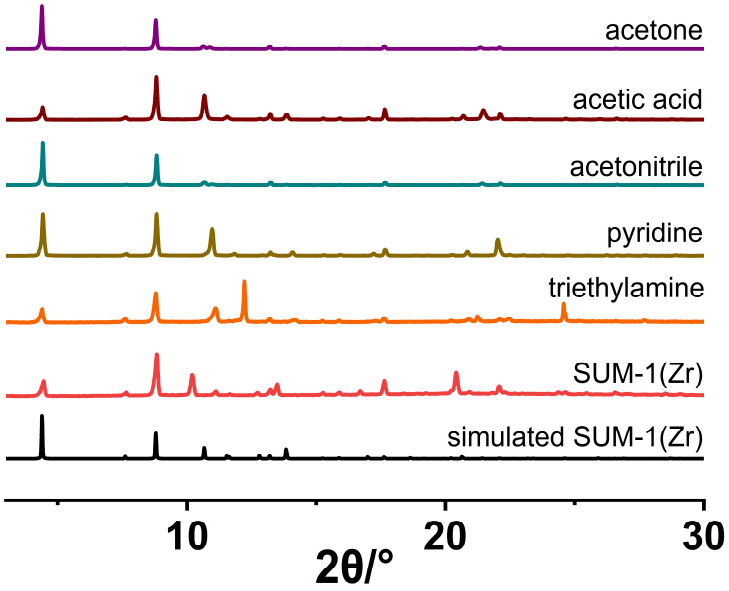

Fig. S34 PXRD patterns of SUM-1(Zr) before (red) and after soaking in various organic solvents for 24 hours, comparing to the simulated pattern (black).

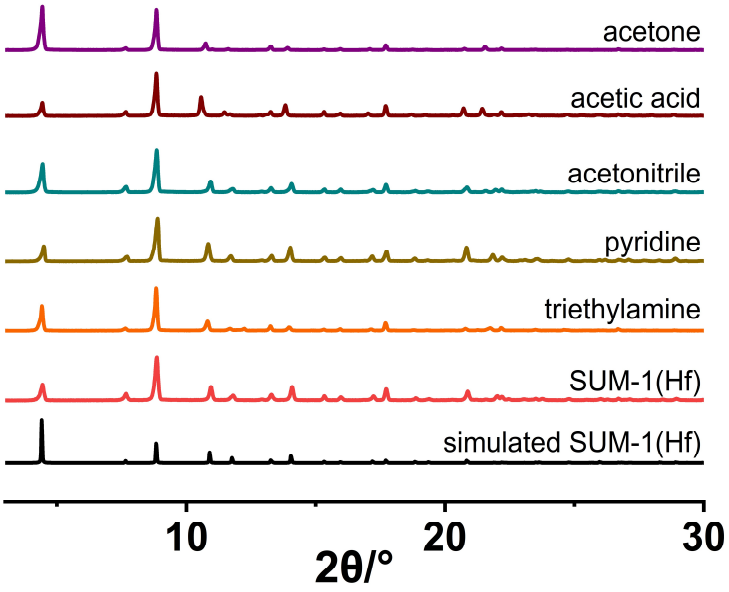

Fig. S35 PXRD patterns of SUM-1(Hf) before (red) and after soaking in various organic solvents for 24 hours, comparing to the simulated pattern (black).

7. Miniaturization of SUM-1(Zr) and characterization

7.1 Synthesis of SUM-1(Zr)-a

H_2-BDHA (6.7 mg, 3.4×10^{-5} mol) was mixed with DMF (1 mL) in a 4-mL glass vial, to which was added concentrated HCl solution (200 μL, 37%) to form a clear solution after sonication. After mixing with a solution of $ZrCl_4$ (2.3 mg, 1×10^{-5} mol) in DMF (1 mL), additional H_2O (400 μL) was added. The open vial was then heated in a 100 ºC isothermal oven for 7 hours. After cooling to room temperature, the crystals were collected and washed with dry DMF.

7.2 Synthesis of SUM-1(Zr)-b

H_2-BDHA (6.7 mg, 3.4×10^{-5} mol) was mixed with DMF (1 mL) in a 4-mL glass vial, to which was added concentrated HCl solution (200 μL, 37%) to form a clear solution after sonication. After mixing with a solution of $ZrCl_4$ (2.3 mg, 1×10^{-5} mol) in DMF (1 mL), additional H_2O (600 μL) was added. The open vial was then heated in a 100 ºC isothermal oven for 7 hours. After cooling to room temperature, the crystals were collected and washed with dry DMF.

7.3 Synthesis of SUM-1(Zr)-c

H_2-BDHA (6.7 mg, 3.4×10^{-5} mol) was mixed with DMF (1 mL) in a 4-mL glass vial, to which was added concentrated HCl solution (200 μL, 37%) to form a clear solution after sonication. After mixing with a solution of $ZrCl_4$ (2.3 mg, 1×10^{-5} mol) in DMF (1 mL), additional H_2O (800 μL) was added. The open vial was then heated in a 100 ºC isothermal oven for 7 hours. After cooling to room temperature, the crystals were collected and washed with dry DMF.

7.4 SEM of SUM-1(Zr)-a, SUM-1(Zr)-b and SUM-1(Zr)-c

Corresponding as-synthesized MOF samples were washed with DMF (3X) and DCM (3X), dried in air at 100 ºC overnight before imaging. Statistics in Fig. 3 of the main text are based on the measurements on the following images.

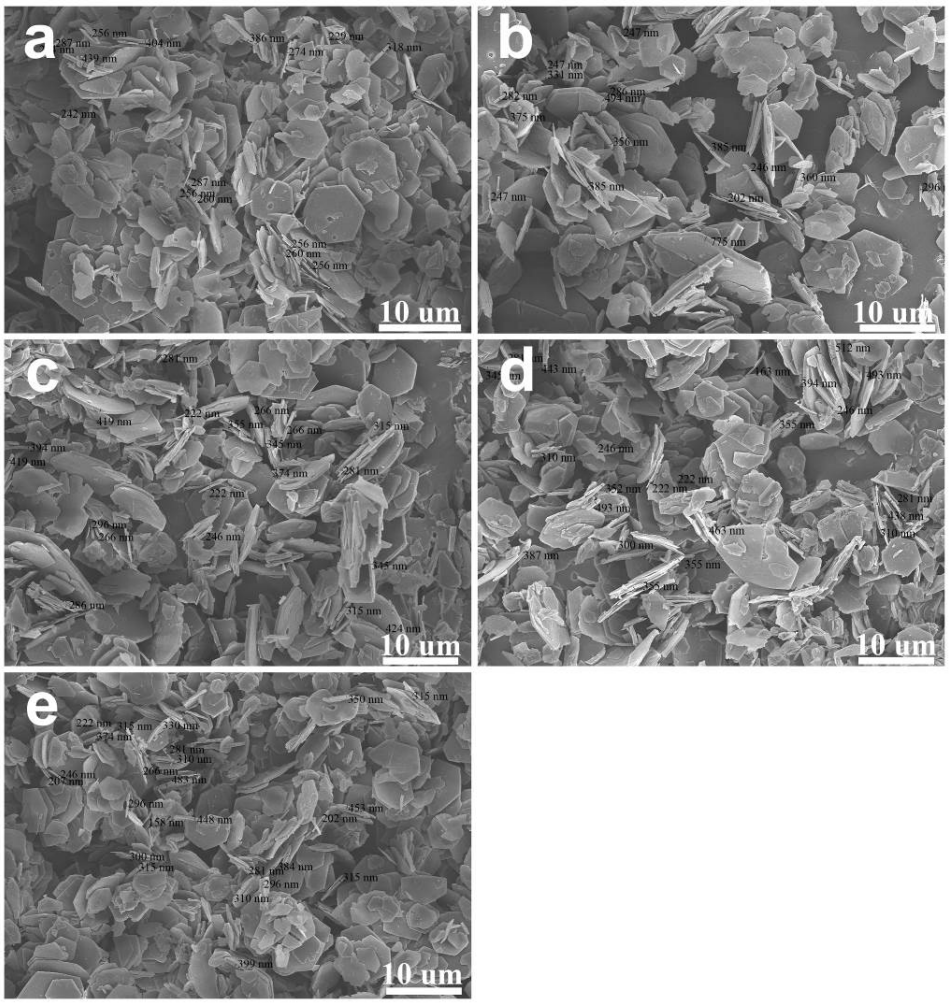

Fig. S36 SEM images of **SUM-1(Zr)-a**, with measurements indicated.

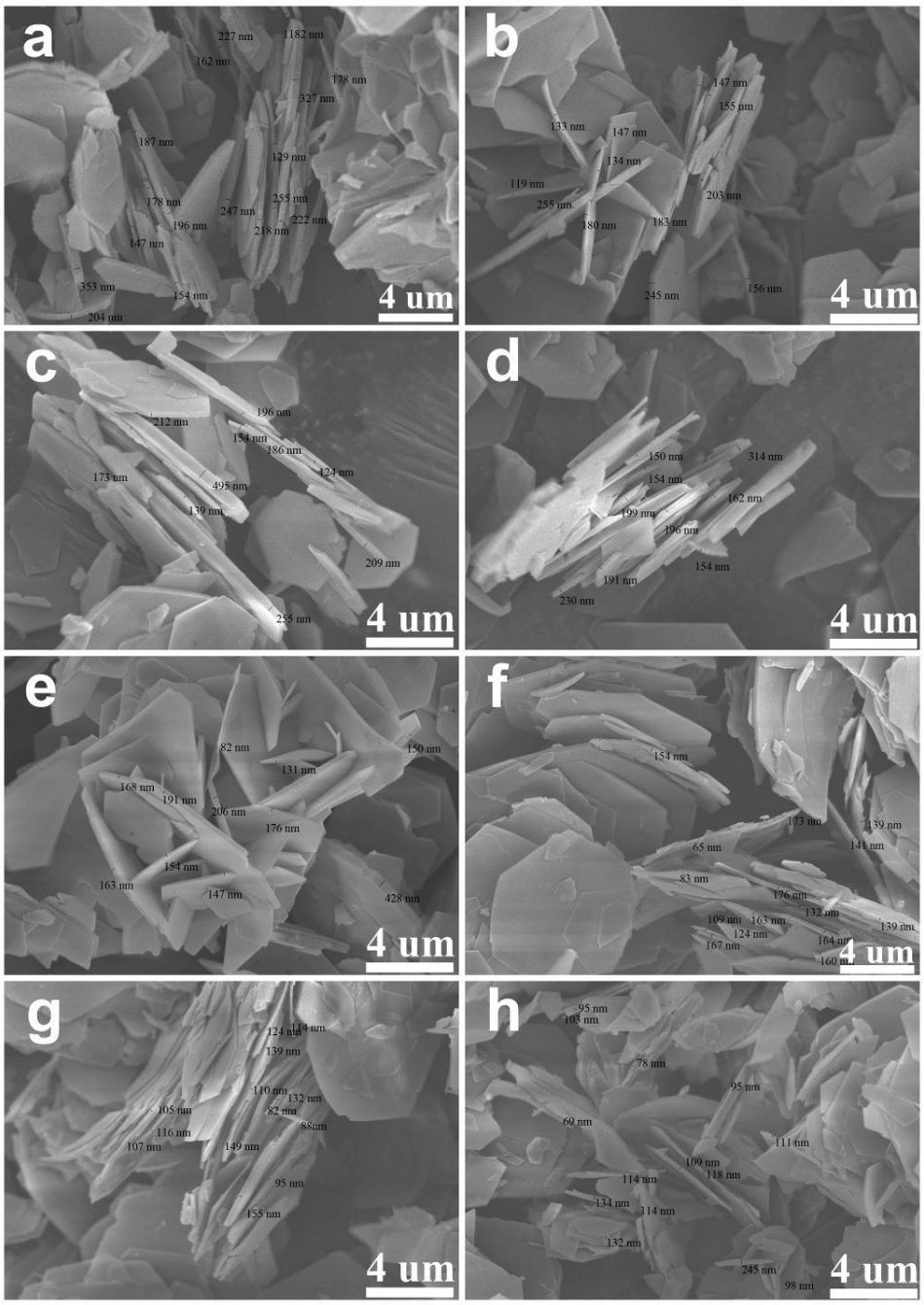

Fig. S37 SEM images of **SUM-1(Zr)-b**, with measurements indicated.

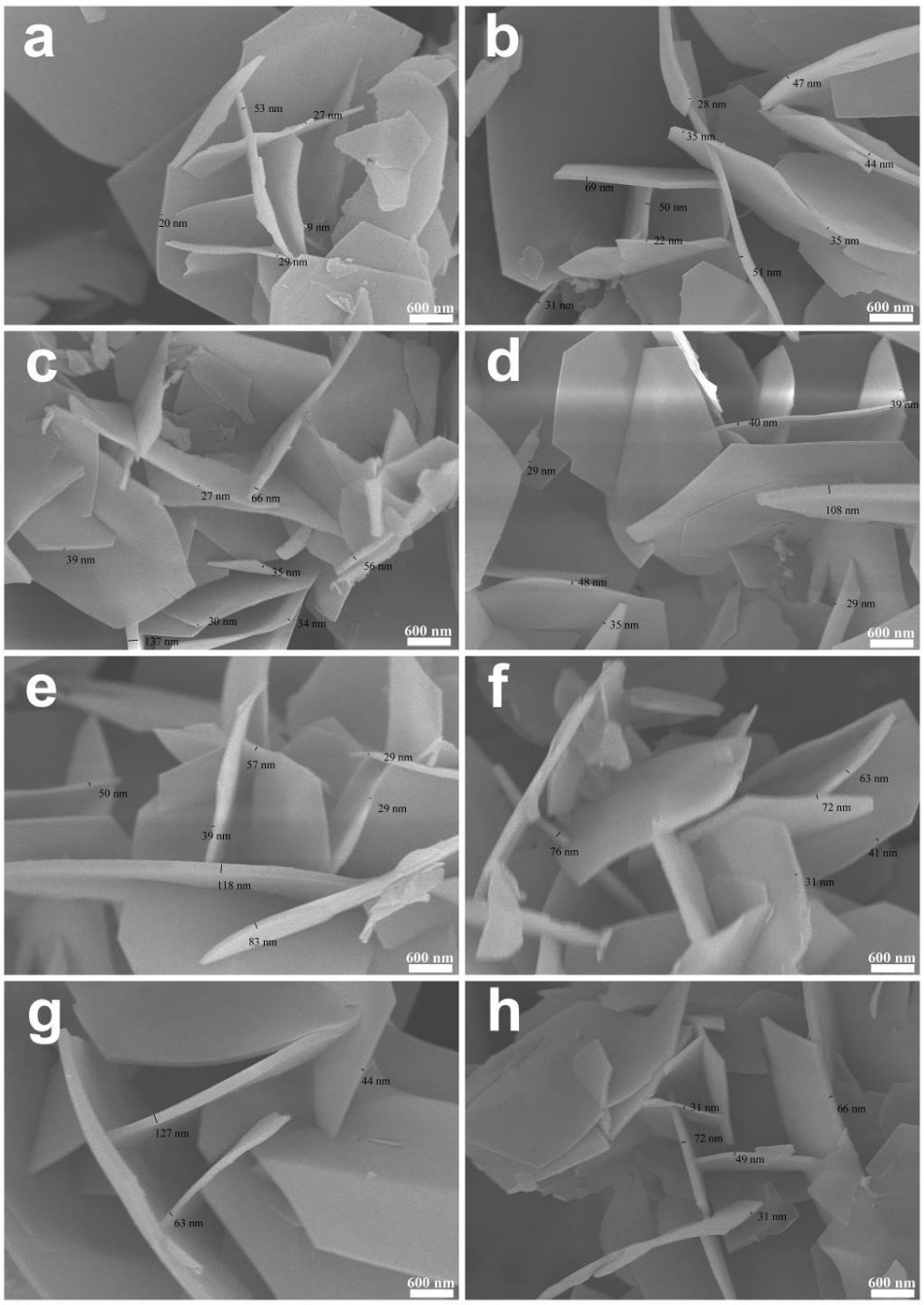

Fig. S38 SEM images of **SUM-1(Zr)-c**, with measurements indicated.

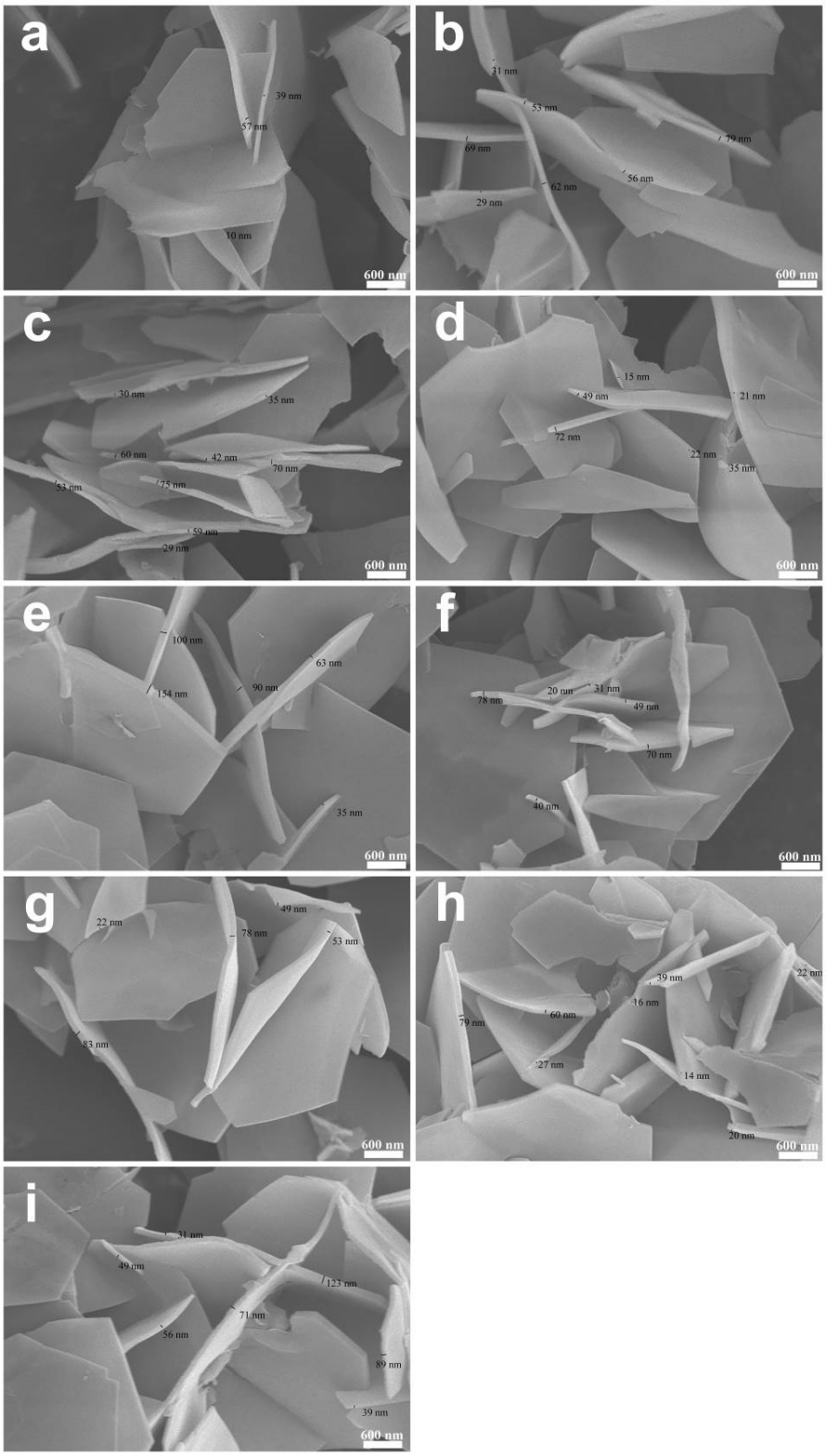

Fig. S39 Additional SEM images of **SUM-1(Zr)-c**, with measurements indicated.

7.5 PXRD of SUM-1(Zr)-a, SUM-1(Zr)-b and SUM-1(Zr)-c

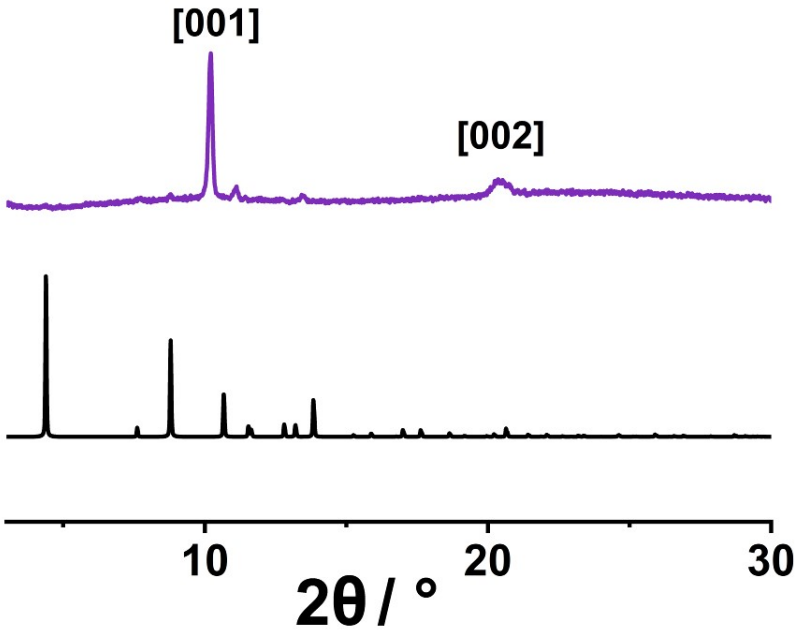

Fig. S40 Experimental PXRD pattern (purple) of as-synthesized SUM-1(Zr)-a comparing to simulated (black) SUM-1(Zr).

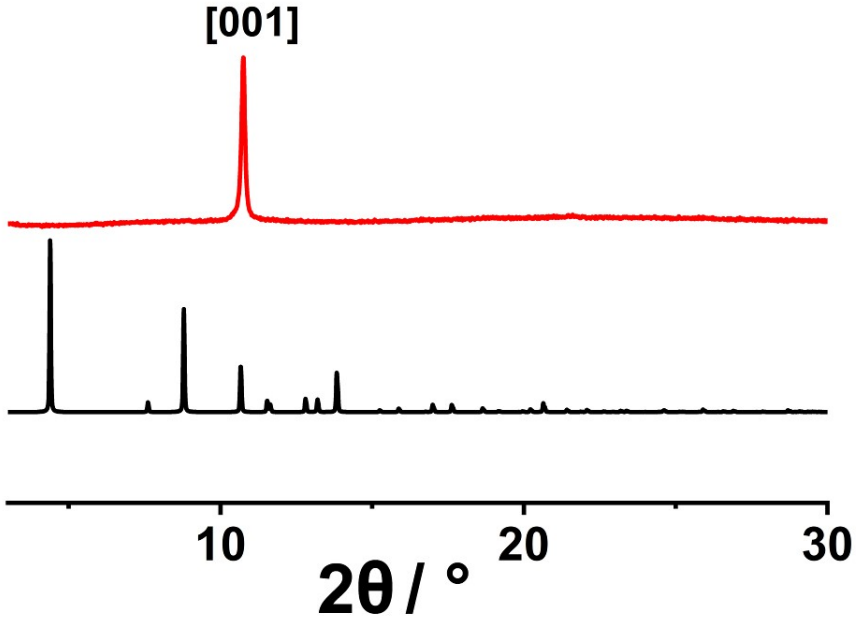

Fig. S41 Experimental PXRD pattern (red) of as-synthesized SUM-1(Zr)-b comparing to simulated (black) SUM-1(Zr).

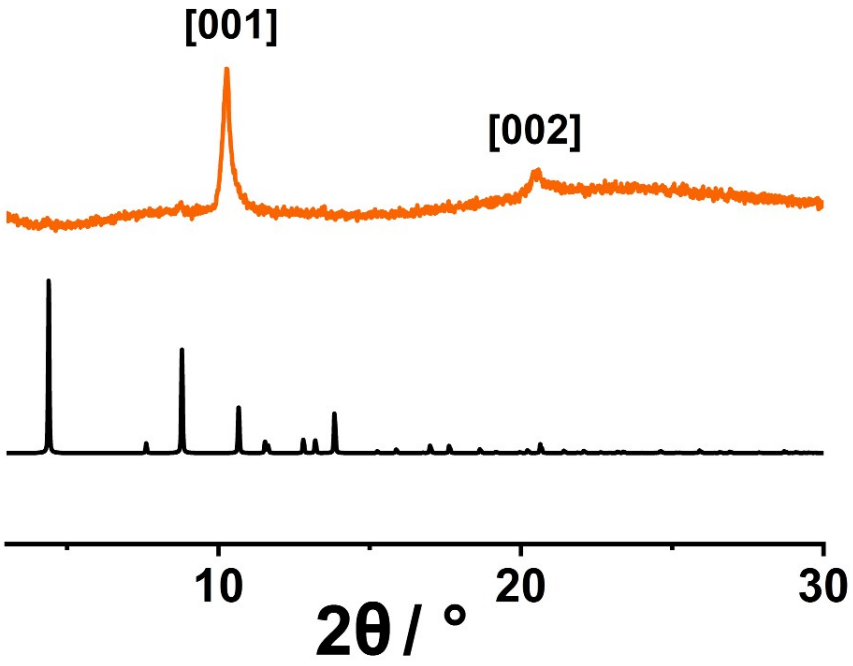

Fig. S42 Experimental PXRD pattern (orange) of as-synthesized SUM-1(Zr)-c comparing to simulated (black) SUM-1(Zr).

7.6 N_2 sorption of SUM-1(Zr)-c

SUM-1(Zr)-c nanoplates were activated using the same procedure for pristine SUM-1(Zr), as described in Section 6.4.

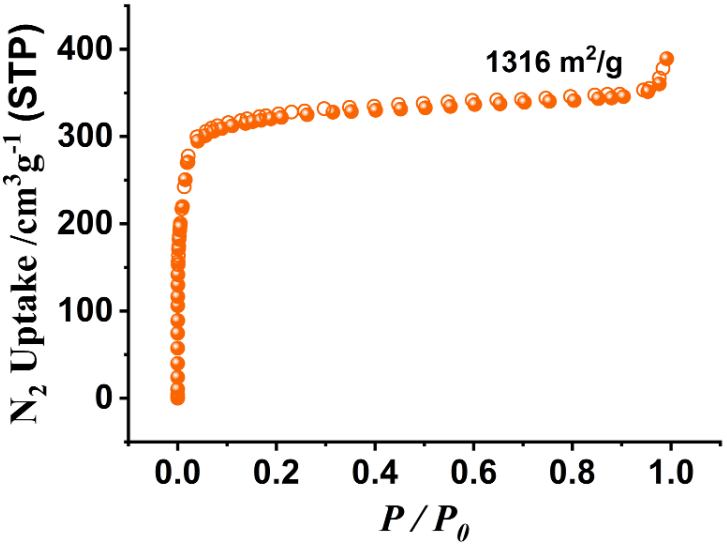

Fig. S43 N_2 adsorption-desorption isotherms of SUM-1(Zr)-c at 77 K (adsorption: filled circles; desorption: open circles).

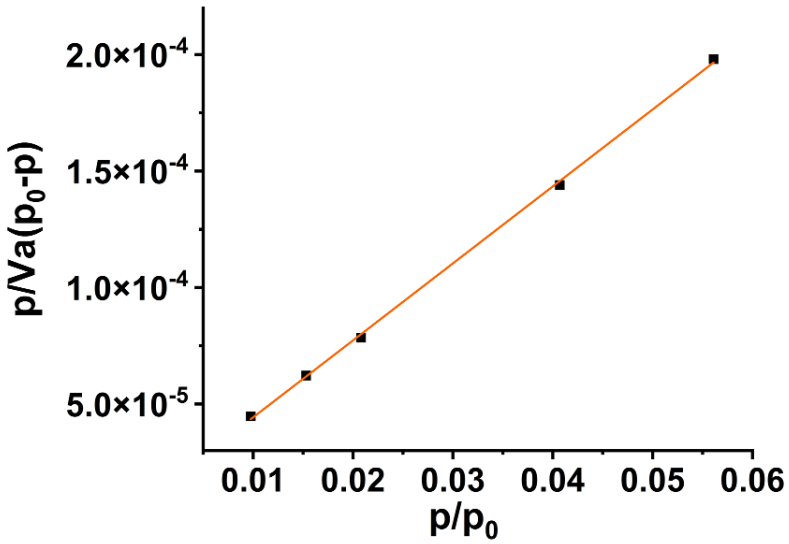

Fig. S44 Multi-point BET plot of SUM-1(Zr)-c.

Table S9 Parameters for SUM-1(Zr)-c calculated from BET analysis

BET Area (m^2g^{-1})	**1316.5**
Slope	**3.2947×10^{-3}**
Intercept	**1.1365×10^{-5}**
R^2	**0.99973**
C	**290.91**
Vm [cm^3(STP)g^{-1}]	**302.47**

7.7 N_2 sorption of SUM-1(Zr)-c after aqueous treatments

As-synthesized SUM-1(Zr)-c nanoplates were washed with dry DMF (3X), then washed (3X) and soaked (24 hours) in aqueous solutions with corresponding pH values. Solutions with different pH were obtained by adding HCl or NaOH. After 24 hours, the samples were activated using acetone, as described in Section 6.4. The results are summarized in Fig. S45-S46 and Table S10.

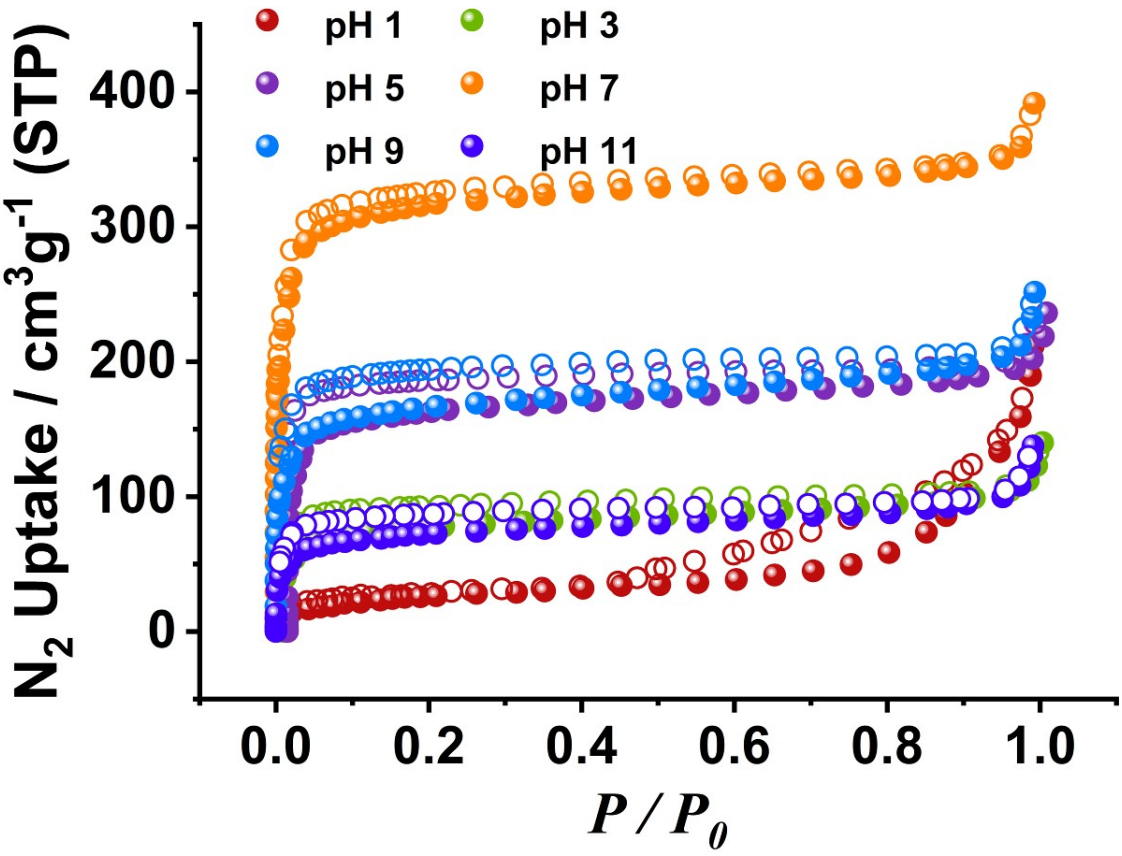

Fig. S45 N_2 adsorption-desorption isotherms of SUM-1(Zr)-c samples at 77 K, after treatments with aqueous solutions of corresponding pH values (adsorption: filled circles; desorption: open circles).

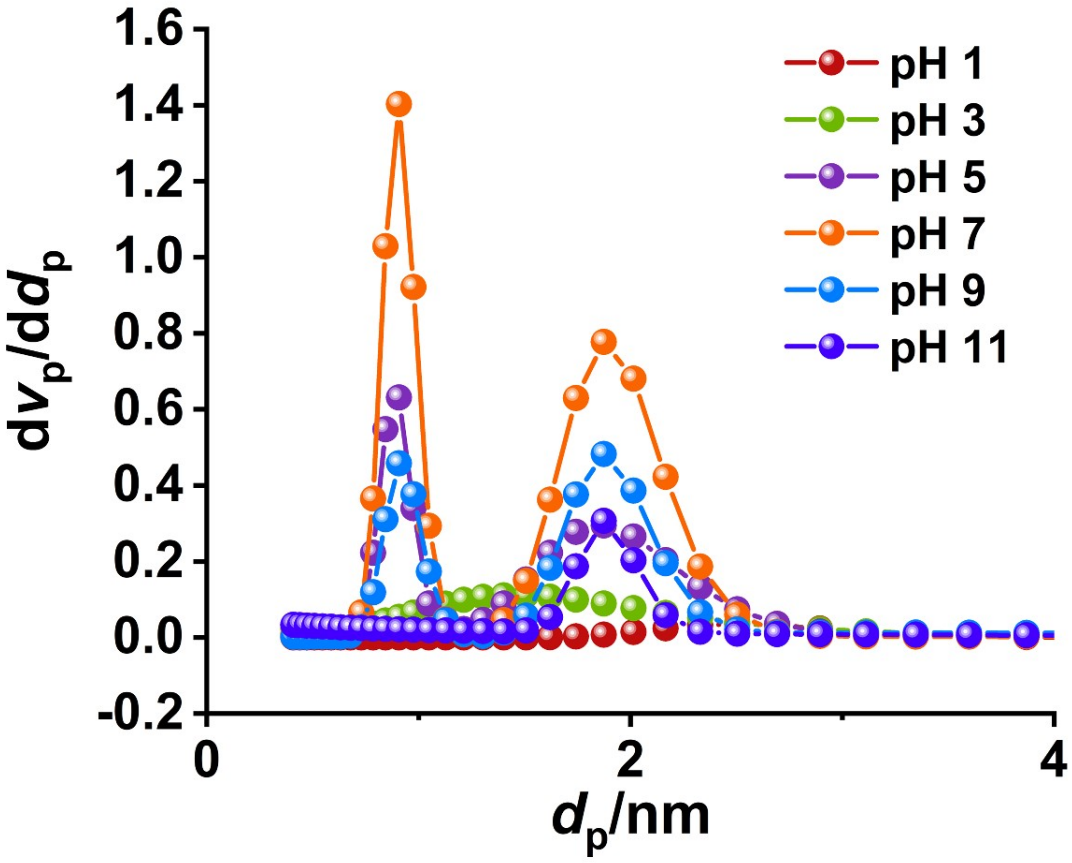

Fig. S46 Pore size distribution plots of various SUM-1(Zr)-c samples based on isotherms in Fig. S43, using the NLDFT method and metal oxides model with cylindrical pores.

Table S10 N_2 uptake and calculated BET area values of various SUM-1(Zr)-c samples based on isotherms in Fig. S43.

SUM-1(Zr)-c	Gas uptake (STP) ($cm^3\ g^{-1}$)	BET area ($m^2\ g^{-1}$)
pH 1	23	100
pH 3	69	300
pH 5	146	633
pH 7	305	1328
pH 9	154	672
pH 11	65	283

References:

(1) Sheldrick, G. *Acta Cryst. Section A.,* **2015**, *71*, 3-8.
(2) Sheldrick, G. *Acta Cryst. Section C.,* **2015**, *71*, 3-8.
(3) Dolomanov, O.V.; Bourhis, L.J.; Gildea, R.J.; Howard, J.A.K.; Puschmann, H. *J. Appl. Cryst.,* **2009**, *42*, 339-341.
(4) Griffith, D.; Krot, K.; Comiskey, J.; Nolan, K. B.; Marmion, C. J. *Dalton Trans.,* **2008**, 137-147.
(5) Hohenberg, P.; Kohn, W. *Phys. Rev.,* **1964**, *136*, B864-B871.
(6) Kohn, W.; Sham, L. J., *Phys. Rev.,* **1965**, *140*, A1133-A1138.
(7) Frisch, M. J.; Trucks, G. W.; Schlegel, H. B.; Scuseria, G. E.; Robb, M. A.; Cheeseman, J. R.; Scalmani, G.; Barone, V.; Petersson, G. A.; Nakatsuji, H.; Li, X.; Caricato, M.; Marenich, A. V.; Bloino, J.; Janesko, B. G.; Gomperts, R.; Mennucci, B.; Hratchian, H. P.; Ortiz, J. V.; Izmaylov, A. F.; Sonnenberg, J. L.; Williams-Young, D.; Ding, F.; Lipparini, F.; Egidi, F.; Goings, J.; Peng, B.; Petrone, A.; Henderson, T.; Ranasinghe, D.; Zakrzewski, V. G.; Gao, J.; Rega, N.; Zheng, G.; Liang, W.; Hada, M.; Ehara, M.; Toyota, K.; Fukuda, R.; Hasegawa, J.; Ishida, M.; Nakajima, T.; Honda, Y.; Kitao, O.; Nakai, H.; Vreven, T.; Throssell, K.; Montgomery, J. A., Jr.; Peralta, J. E.; Ogliaro, F.; Bearpark, M. J.; Heyd, J. J.; Brothers, E. N.; Kudin, K. N.; Staroverov, V. N.; Keith, T. A.; Kobayashi, R.; Normand, J.; Raghavachari, K.; Rendell, A. P.; Burant, J. C.; Iyengar, S. S.; Tomasi, J.; Cossi, M.; Millam, J. M.; Klene, M.; Adamo, C.; Cammi, R.; Ochterski, J. W.; Martin, R. L.; Morokuma, K.; Farkas, O.; Foresman, J. B.; Fox, D. J. *Gaussian 16, rev. B.01*; Gaussian, Inc.: Wallingford, CT, **2016**.
(8) Becke, A. D. *Phys. Rev. A: At., Mol., Opt. Phys.,* **1988**, *38*, 3098-3100.
(9) Lee, C.; Yang, W.; Parr, R. G. *Phys. Rev. B: Condens. Matter Mater. Phys.,* **1988**, *37*, 785-789.
(10) Krishnan, R.; Binkley, J. S.; Seeger, R.; Pople, J. A. *J. Chem. Phys.,* **1980**, *72*, 650-654.
(11) McLean, A. D.; Chandler, G. S. *J. Chem. Phys.,* **1980**, *72*, 5639-5648.
(12) Dolg, M.; Peterson, K. A.; Schwerdtfeger, P.; Stoll, H. *Pseudopotentials of the Stuttgart/Cologne Group,* **2014**. http://www.tc.uni-koeln.de/PP/clickpse.en.html.
(13) Cavka, J. H.; Jakobsen, S.; Olsbye, U.; Guillou, N.; Lamberti, C.; Bordiga, S.; Lillerud, K. P. *J. Am. Chem. Soc.,* **2008**, *130*, 13850-13851.
(14) Katz, M. J.; Brown, Z. J.; Colón, Y. J.; Siu, P. W.; Scheidt, K. A.; Snurr, R. Q.; Hupp, J. T.; Farha, O. K. *Chem. Commun.,* **2013**, *49*, 9449-9451.
(15) Goesten, M. G.; de Lange, M. F.; Olivos-Suarez, A. I.; Bavykina, A. V.; Serra-Crespo, P.; Krywka, C.; Bickelhaupt, F. M.; Kapteijn F.; Gascon, J. *Nat. Commun.*, **2016**, *7*, 11832.
(16) Padial, N. M.; Castells-Gil, J.; Almora-Barrios, N.; Romero-Angel, M.; da Silva, I.; Barawi, M.; García-Sánchez, A.; de la Peña O'Shea, V. A.; Martí-Gastaldo, C. *J. Am. Chem. Soc.,* **2019**, *141*, 13124-13133.